McCarthy, B. J., and Holland, J. J. (1965), *Proc. Natl. Acad. Sci. U. S. 54*, 880.
Nakada, D. (1965), *J. Mol. Biol. 12*, 695.
Nirenberg, M. W. (1964), *Methods Enzymol. 6*, 17.
Nirenberg, M. W., and Matthaei, J. H. (1961), *Proc. Natl. Acad. Sci. U. S. 47*, 1588.
Otaka, E., Osawa, S., and Sibatani, A. (1964), *Biochem. Biophys. Res. Commun. 15*, 568.
Siekevitz, P. (1952), *J. Biol. Chem. 195*, 549.
So, A. G., Bodley, J. W., and Davie, E. W. (1964), *Biochemistry 3*, 1977.
Speyer, J. F., Lengyel, P., and Basilio, C. (1962), *Proc. Natl. Acad. Sci. U. S. 48*, 684.
Spotts, C. R., and Stanier, R. Y. (1961), *Nature 192*, 633.
Srinivasan, P. R., and Borek, E. (1964), *Science 145*, 548.
Tissières, A., Schlessinger, D., and Gros, J. (1960), *Proc. Natl. Acad. Sci. U. S. 46*, 1450.
Von Ehrenstein, G., and Lipmann, J. (1961), *Proc. Natl. Acad. Sci. U. S. 47*, 941.

Comparison of Experimental Binding Data and Theoretical Models in Proteins Containing Subunits*

D. E. Koshland, Jr.,† G. Némethy, and D. Filmer

ABSTRACT: Models for subunit interactions are examined by means of interpreting ligand saturation curves. Equations are derived to indicate the effect of variables such as the strength of binding of the ligand, the geometrical arrangement of subunits, the strength of interaction between subunits, the energy of the conformation change, and the effect of nonidentical subunits. Rapid methods, *i.e.*, equations and nomograms, are developed to fit theoretical curves to experimental data with a minimum of parameters. Applying these procedures to the binding of oxygen by hemoglobin as an illustrative example, it is seen that a number of simple models can represent the published data accurately. In general it appears that unique mechanisms cannot be established from ligand saturation curves by themselves, but the mathematical analysis of the curves indicates possible sources of additional information to make such distinctions possible.

For many years it has been known that the binding of oxygen to hemoglobin follows a sigmoid curve which differs appreciably from the typical Michaelis–Menten equation covering the same concentration range. An empirical equation designed by Hill (1910), $Y = kp^n/(1 + kp^n)$, gave a reasonable approximation to the data with $n \approx 2.6$. Adair (1925) obtained a closer fit using a four-constant equation in which the constants related the successive affinity constants of oxygen to the four heme groups in hemoglobin. Adair's equation did not provide any theoretical explanation for the changing affinity constants, but it was capable of fitting the data quite accurately. Pauling (1935) made the first attempt to relate the change in these constants to the geometry of the protein by assuming a single affinity constant and an interaction term which depended on the geometry of the four subunits. Excellent recent reviews on linked functions and binding of hemoglobin have been presented by Wyman (1964) and Rossi-Fanelli *et al.* (1964).

The recent emphasis on the properties of proteins has highlighted the importance of the hemoglobin problem in several ways. In the first place, protein conformational changes provide perhaps the best explanation for the "interaction" between heme groups during the binding of oxygen. This hypothesis is supported by the elegant studies of Perutz and co-workers (1964) who found that the hemes lie far from each other in the hemoglobin molecule and that a conformational change apparently occurs when oxygen is absorbed to hemoglobin. In the second place, the widespread observation of conformational effects in enzyme systems in general and in regulatory systems in particular together with the observation that most of these enzymes are composed of subunits indicates that the hemoglobin interactions may not be an isolated phenomenon but rather one manifestation of a general situation (Grisolia, 1964; Umbarger, 1964; Gerhart and Pardee, 1962; Monod *et al.*, 1963; Koshland, 1963).

Monod *et al.* (1965) have recently proposed an interesting new model to explain the hemoglobin satura-

* From the Biology Department, Brookhaven National Laboratory, Upton, New York 11973, and The Rockefeller Institute, New York, New York 10021. *Received August 2, 1965.* A portion of the research was carried out at Brookhaven National Laboratory under the auspices of the U. S. Atomic Energy Commission. This work was also supported by the National Science Foundation.

† Present address: Department of Biochemistry, University of California, Berkeley, Calif.

tion curve. This model postulates that a protein composed of subunits must maintain symmetry during conformational changes. From this they deduce that the protein must exist in two forms, one of which contains all the subunits in one conformation, the other with all the subunits in a second conformation. With this model and the assumption that one form can bind O_2 more strongly than the other they are able to fit the O_2 binding data of L. Lyster (quoted in Monod *et al.*, 1965) very satisfactorily and predict that this may be a plausible model for control enzymes in general.

Atkinson and co-workers (1965) have also proposed an important model for ligand interactions which differs significantly from the model of Monod *et al.* (1965). In the cases of the enzymes phosphofructokinase and isocitrate dehydrogenase they find complex relationships between substrates and modifiers and are able to explain these results by a model which assumes progressive changes in ligand site interactions. In this model binding of ligand at one site can either increase or decrease the affinity of ligand at a second site, which can in turn affect the binding of ligand at a third site, etc.

These significant studies and the mounting literature on subunits and conformations led us to an examination of interrelationships of conformational effects and subunits. One of the particular difficulties in this area is the comparison of experimental data with theoretical models. It is already laborious to determine whether a given model is consistent with experimental data. Unless simplified procedures are available it is even worse to compare a variety of models to establish unique mechanisms. It seemed appropriate, therefore, to approach such questions as "How can experimental data be fitted simply and systematically to the predictions of theoretical models?" "Can more than one model satisfy a given saturation curve?" "Can theoretical derivations indicate what additional parameters should be investigated to distinguish between models?"

A cursory examination demonstrated that the number of potential models was very large. Therefore, it was decided to attempt to answer these questions in the framework of a model involving four subunits, one binding site per subunit, and one type of ligand. Not only would such a model be applicable to hemoglobin on which such extensive work has already been performed, but also the single structure found most frequently among enzymes involves four similar subunits (Schachman, 1963). Variables that were investigated included the geometrical relationship of subunits, the binding constant of ligand to protein, the strength of interaction between subunits, and the effect of nonidentical subunits. The appropriate equations for various models were derived and the effect of individual parameters on the shapes of these saturation curves was established with the aid of a computer. The relationships obtained made it possible to develop a systematic procedure for fitting an experimental saturation curve to the calculated curves of a theoretical model. The procedure so developed was then applied to hemoglobin to determine which, if any, models fitted the data satisfactorily. The fitting of the data to hemoglobin and the comparison of the theoretical curves with each other made it possible to ascertain which of the intrinsic constants could be distinguished by saturation curves and what additional data would be required to obtain unique mechanisms. Although the approach is applied to a four-subunit protein in this paper for illustrative purposes, it is clear that the methods are readily applicable to other systems, containing differing numbers of subunits.

Definition of Terms. In all the models it will be assumed that the individual subunits of the protein can exist in two conformations, A and B, and that only conformation B binds the ligand S in significant amounts. Since the mathematics involves ES interactions, it applies directly to compounds which are bound, but do not react, such as oxygen binding to hemoglobin or inhibitors in enzyme systems. It would also apply to enzyme–substrate complexes when the amount of the ES complex is directly related to a measurable property such as activity. For example, an enzyme system in which the ES complex decomposes in such a way that the activity is proportional to the amount of the ES complex would give an activity–substrate concentration curve similar to the saturation curve.

The substrate binding constant K_s represents the intrinsic affinity of the ligand for an individual subunit and is defined according to eq 1.

$$K_s = \frac{(BS)}{(B)(S)} \tag{1}$$

The transformation constant K_t represents the equilibrium constant for the conformation change from the subunit in conformation A to the subunit in conformation B, as shown in eq 2.

$$K_t = \frac{(B)}{(A)} \tag{2}$$

This constant does not include the effect of changing interactions of subunits.

To represent the interaction between subunits of different conformational structure, the constants K_{AA}, K_{AB}, and K_{BB} will be employed.[1] In this connection it will be assumed that $K_{AA} = 1$ since a choice of any other number would simply reflect a relative shift in the standard state, rather than a significant change in the subunit relationships. K_{AB} and K_{BB} are defined by eq 3 and 4 in which (AB) refers to interacting subunits, whereas (A) and (B) refer to noninteracting subunits.

$$K_{AB} = \frac{(AB)(A)}{(AA)(B)} \tag{3}$$

[1] Some of the relationships between constants of this type have been discussed by Coryell (1939).

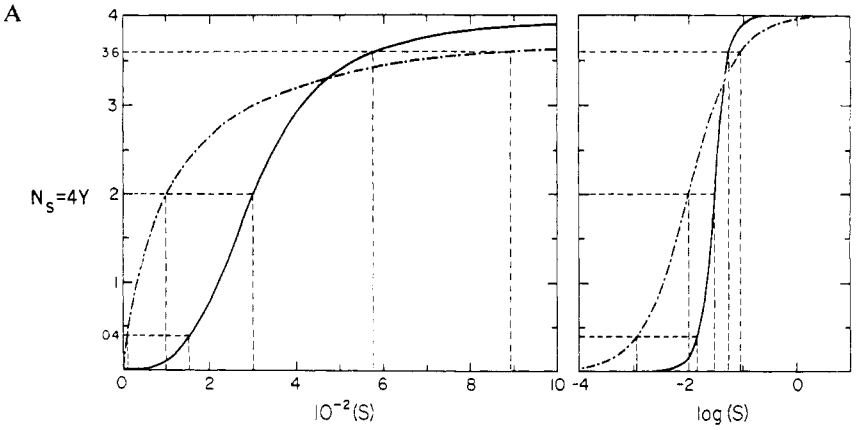

FIGURE 1: Comparison of a sigmoid saturation curve (———) with a Michaelis–Menten saturation curve (–·–·–·–). (A) Plotting N_s *vs.* (S) and (B) on a plot of N_s *vs.* log (S). On both plots, the levels of saturation (N_s = 0.4, 2.0, and 3.6, corresponding to 10, 50, and 90% saturation, respectively) used to define the characteristic parameters ($S_{0.5}$) and R_s, and the concentrations corresponding to each, are indicated by dashed lines.

$$K_{BB} = \frac{(BB)(A)(A)}{(AA)(B)(B)} \qquad (4)$$

It is to be noted that eq 3 and 4 contain equal stoichiometric amounts of A and B in numerator and denominator and, therefore, the equilibrium constants in these expressions relate to the changes in the strengths of interaction between subunits and do not contain the energy of the conformation change itself. Thus, these constants represent the increased ($K > 1$) or decreased ($K < 1$) stabilization of some conformations of the protein brought about by the interaction of subunits. For example, $K_{AB} > 1$ means that the interaction of AB is more favorable than the interaction of AA and tends to stabilize an AB neighbor with respect to an AA pair.

For the "concerted" case the constants K_t, K_{AB}, K_{BB}, etc., can be expressed as a single constant, K_{tc}. Because an understanding of the meaning of this constant requires a description of the model, its definition is deferred to eq 25.

The symbol Y is used to represent the fraction of binding sites occupied and can vary from 0 to 1.0 (Pauling, 1935). The symbol N_s represents the average number of molecules of substrate bound per molecule of enzyme as defined by eq 5, where i represents the number of molecules of S bound to an individual molecular species and n represents the number of subunits per molecular species. It is clear that both N_s and i can range from 0 to n, but i can have only integral values, whereas N_s can have fractional values.

$$N_s = nY = \frac{\text{(substrate bound)}}{\text{(total enzyme)}} = \frac{\sum_{i=1}^{i=n} i(ES_i)}{\sum_{i=0}^{i=n} (ES_i)} \qquad (5)$$

If the subunits are not identical but exist, for example, in two pairs two types of subunit interactions may exist. One illustrative example would be an interaction of the "head" of the α chain with the "tail" of the β chain as compared to the interaction of the tail of the α chain with the head of the β chain. The added complications of this case will be discussed later.

We shall generally refer to Y *vs.* (S), N_s *vs.* (S), or N_s *vs.* log (S) plots as "saturation curves." For ease of presentation, the N_s nomenclature will be used in this paper to emphasize the protein contains four subunits, although the Y nomenclature is more general and may be preferred in other situations. Interconversion to the Y system is readily achieved from the relation $N_s = 4Y$.

In Figure 1A a typical sigmoid curve is compared to a classical Michaelis–Menten curve covering the same concentration range. In Figure 1B the same two curves are plotted on a log (S) plot in which case both curves are sigmoid. In comparing theory and experiment it will be useful to characterize these curves with two constants illustrated in the figure. ($S_{0.5}$) will be used to refer to the value of (S) when $Y = 0.5$, *i.e.*, when half the sites are saturated with ligand. R_s will be used to refer to the ratio of ligand concentration at $Y = 0.9$, *i.e.*, at 90% saturation, relative to the ligand concentration when $Y = 0.1$, *i.e.*, at 10% saturation (*cf.* eq 6). The symbol R_s serves not only to aid the choice of a theoretical curve but allows an immediate comparison to Michaelis–Menten behavior since $R_s = 81(S_{0.5})$ for any system following the Michaelis–Menten equation. Obviously these ratios will indicate the sharpness of the N_s–log (S) curve, *i.e.*, the curve will be steeper when a smaller change in (S) is required to convert from an average of 10% saturation to an average of 90% saturation. Thus an R_s value less than 81 indicates a curve which is steeper than a Michaelis–Menten curve.

In some experimental situations it will be desirable to compare points at greater extremes, *e.g.*, ($S_{0.975}$), or at intermediate positions, *e.g.*, ($S_{0.8}$). In these cases R_s',

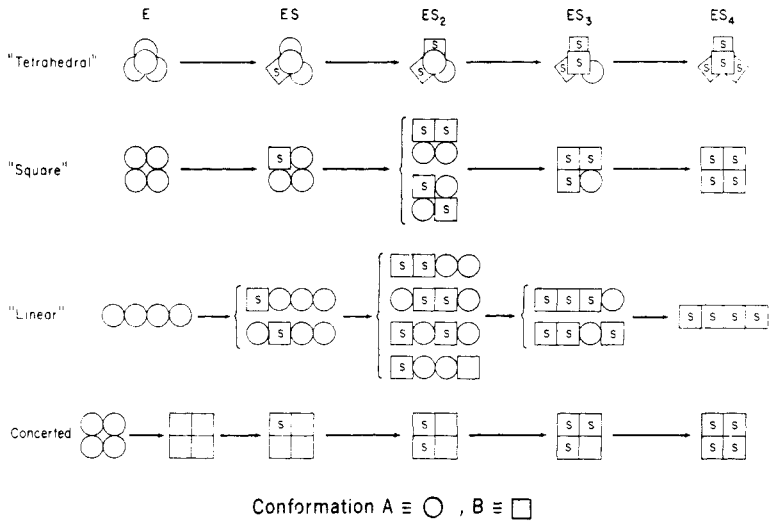

FIGURE 2: Schematic illustration of the various modes of binding the ligand S to the tetrameric enzyme for the four major cases discussed in this paper. Conformation A of the subunit is denoted by circles. Conformation B, the one capable of binding S, is denoted by squares. In the models involving a progressive change it is assumed that a subunit in conformation B is present only when S is bound to it. In the concerted model all conformations change to B together.

R_s'', etc., can be defined as desired. In this article we shall define R_s and R_s' as shown in eq 6.

$$R_s = \frac{(S_{0.9})}{(S_{0.1})} = \frac{\text{substrate concentration when } N_s = 3.6}{\text{substrate concentration when } N_s = 0.4} \qquad (6)$$

$$R_s' = \frac{(S_{0.975})}{(S_{0.025})} = \frac{\text{substrate concentration when } N_s = 3.9}{\text{substrate concentration when } N_s = 0.1}$$

R_a will be used to indicate the symmetry of the saturation curve around the mid-point and is to be calculated from the ratios of ligand concentrations at $Y = 0.9$, 0.1, and 0.5, as shown in eq 7. The parameter R_a' can be defined in an analogous way.

$$R_a = \frac{(S_{0.9})(S_{0.1})}{(S_{0.5})^2} \qquad (7)$$

The ratio R_a will obviously equal 1.0 for a curve which is symmetrical about $Y = 0.5$. From Figure 1 the symmetry is visually apparent in the N_s *vs.* log (S) plots but not in the N_s *vs.* (S) plot. Of course, R_a (or any similar ratio, *e.g.*, R_a') can be calculated from either curve. As will be apparent later, the choice of R_s and R_a or R_s' and R_a' may depend on the data that are available.

The Models. For this paper a limited number of models of subunit interactions will be evaluated. All interactions will be assumed to occur in a single protein containing four subunits. For convenience in visualizing these effects a geometrical designation of the subunit interactions is helpful, and the various models will be referred to by descriptive phrases such as "tetrahedral," "square," "linear," etc., following the nomenclature suggested by Pauling (1935) (*cf.* Figure 2).

The terms "tetrahedral," "square," etc. are used to clarify the permissible subunit interactions and do not necessarily correspond to the actual arrangement of the subunits in three-dimensional space. For example, the tetrahedral case assumes that each subunit can interact with each of the other three subunits. This mathematical relationship could be satisfied either by a tetrahedral array of subunits or by a square arrangement of subunits in which diagonal interactions were allowed. Conversely, a tetrahedral geometry in which certain subunit interactions were excluded might give a final mathematical result describable by the square model. This would be the case for a molecule of 2α and 2β chains arranged in a tetrahedral geometry in which only α,β interactions occurred.

In Figure 2 schematic representations of the four major cases we will consider are represented utilizing identical subunits. In the tetrahedral case each subunit presumably interacts with each of the other subunits. In the square case the subunits are arranged so that each subunit interacts with each of two neighbors, it being presumed that diagonal interactions are negligible. In the linear case it is assumed that there is no interaction between terminal subunits and, therefore, that the interior subunits each interact with two neighbors

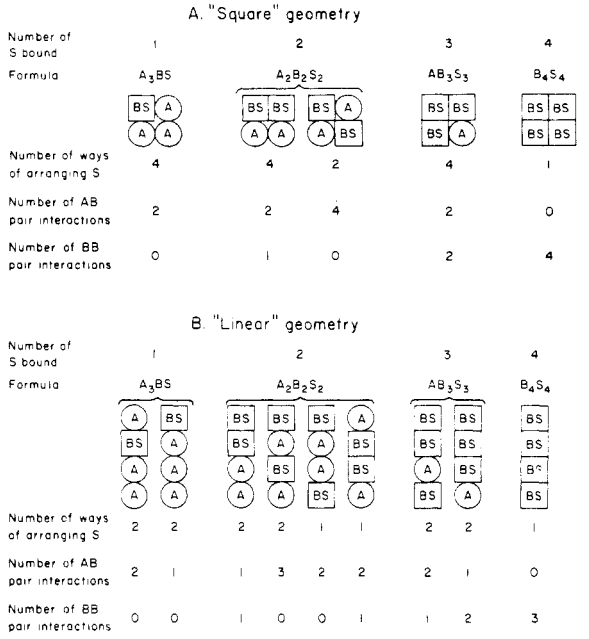

FIGURE 3: Schematic illustration of the various modes of binding and the number of subunit interactions for (a) the "square," (b) the "linear" geometry. Notation for the various forms of the subunits is the same as in Figure 2.

whereas the two terminal units interact only with one neighbor. The concerted case is represented in a square array merely for convenience, but this model does not depend on the geometry of the interactions since all subunits change simultaneously. The allosteric model of Monod *et al.* (1965) utilizes such a concerted change but also assumes various symmetry requirements which are not an essential part of the concerted model shown here.

In the case of the square and linear cases there is more than one type of interaction when two substrate molecules are bound, whereas in the tetrahedral and concerted cases there is only one distinguishable arrangement provided the subunits are identical (Figure 2). Statistical weight of the various forms will be discussed below.

Derivation of Binding Equations. If there is no interaction between subunits the degree of polymerization of the protein is irrelevant and the saturation curve will follow a typical adsorption isotherm such as the Michaelis–Menten kinetic equation (1913). In terms of the constants derived above, this would have the form of eq 8.

$$N_s = \frac{4K_sK_t(S)}{1 + K_sK_t(S)} \tag{8}$$

When subunit interactions can occur the relationship of binding and interactions of subunits is much more complex. A schematic illustration of the conformation changes is shown in Figure 2. In Figure 3 some of the details of interactions of the square and linear cases are outlined for illustrative purposes.

"Tetrahedral" Model. A tetrahedral arrangement results in four equivalent ways to bind one molecule of (S), six ways to bind two, four ways to bind three, and one way to bind four. The number of interacting pairs will be 3 A–B and 3 A–A for the A_3BS species; 1 B–B, 4 A–B, and 1 A–A for $A_2B_2S_2$; 3 B–B and 3 A–B for AB_3S_3; and 6 B–B for B_4S_4. When $K_{AB} \neq 1$ and K_{BB}

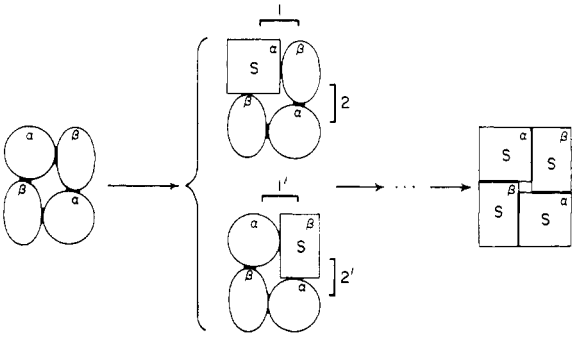

FIGURE 4: Schematic illustration of some relationships when nonidentical subunits are present. A case analogous to the "square" geometry is shown in which only forms E, ES, and ES_4 are presented. Subunits in form A are denoted by circles or ellipses, subunits in form B by squares or rectangles. It is assumed that the enzyme consists of two pairs of identical subunits, denoted by α (circles or squares) and β (ellipses or rectangles). Note that there are two possible forms of ES, with different interactions (indicated by brackets). In the case of unequal interactions, the α,β interactions, 1′ and 2′, differ from each other and from interaction 1.

$\neq 1$, the concentrations of enzyme molecules binding a given number of S molecules bound are given by eq 9–12. Substituting these equations into eq 5 the relationship for N_s shown in eq 13 is obtained.

$$(ES) = (A_3BS) = 4K_{AB}{}^3[K_sK_t(S)](A_4) \tag{9}$$

$$(ES_2) = (A_2B_2S_2) = 6K_{AB}{}^4K_{BB}[K_sK_t(S)]^2(A_4) \tag{10}$$

$$(ES_3) = (AB_3S_3) = 4K_{AB}{}^3K_{BB}{}^3[K_sK_t(S)]^3(A_4) \tag{11}$$

$$(ES_4) = (B_4S_4) = K_{BB}{}^6[K_sK_t(S)]^4(A_4) \tag{12}$$

$$N_s = \frac{4K_{AB}{}^3[K_sK_t(S)] + 12K_{AB}{}^4K_{BB}[K_sK_t(S)]^2 + 12K_{AB}{}^3K_{BB}{}^3[K_tK_s(S)]^3 + 4K_{BB}{}^6[K_tK_s(S)]^4}{1 + 4K_{AB}{}^3[K_sK_t(S)] + 6K_{AB}{}^4K_{BB}[K_sK_t(S)]^2 + 4K_{AB}{}^3K_{BB}{}^3[K_sK_t(S)]^3 + K_{BB}{}^6[K_sK_t(S)]^4} \tag{13}$$

$$(ES) = (A_3BS) = 4K_{AB}^2[K_sK_t(S)](A_4) \quad (14)$$

$$(ES_2) = (A_2B_2S_2) = (4K_{AB}^2K_{BB} + 2K_{AB}^4)[K_sK_t(S)]^2(A_4) \quad (15)$$

$$(ES_3) = (AB_3S_3) = 4K_{AB}^2K_{BB}^2[K_sK_t(S)]^3(A_4) \quad (16)$$

$$(ES_4) = (B_4S_4) = K_{BB}^4[K_sK_t(S)]^4(A_4) \quad (17)$$

When $K_{AB} = 1$ and $K_sK_t = K_p'$, this equation reduces to the tetrahedral case equation derived by Pauling (1935).

"*Square*" *Case.* The square case assumes four subunits in a square pattern in which no interactions across the diagonal occur. The number of ways of binding S and the number of AB and BB pair interactions are given in Figure 3. The concentration of the various species are given by eq 14–17 and the values of N_s by eq 18. When $K_{AB} = 1$ and $K_{BB} > 1$, this equation reduces to the square case equation derived by Pauling (1935) for hemoglobin.

$$N_s = \frac{4K_{AB}^2[K_sK_t(S)] + 4(K_{AB}^4 + 2K_{AB}^2K_{BB})[K_sK_t(S)]^2 + 12K_{AB}^2K_{BB}^2[K_sK_t(S)]^3 + 4K_{BB}^4[K_sK_t(S)]^4}{1 + 4K_{AB}^2[K_sK_t(S)] + (2K_{AB}^4 + 4K_{AB}^2K_{BB})[K_sK_t(S)]^2 + 4K_{AB}^2K_{BB}^2[K_sK_t(S)]^3 + K_{BB}^4[K_sK_t(S)]^4} \quad (18)$$

$$N_s = \frac{4K_{AB}^2[K_sK_t(S)] + 4(K_{AB}^4 + 2K_{AB}^2)[K_sK_t(S)]^2 + 12K_{AB}^2[K_sK_t(S)]^3 + 4[K_sK_t(S)]^4}{1 + 4K_{AB}^2[K_sK_t(S)] + (2K_{AB}^4 + 4K_{AB}^2)[K_sK_t(S)]^2 + 4K_{AB}^2[K_sK_t(S)]^3 + [K_sK_t(S)]^4} \quad (19)$$

An interesting case occurs when $K_{AB} \neq 1$ and $K_{BB} = 1$. These assumptions require that the interactions between AA conformations are the same as the interactions between BB conformations but are different from the interactions between the two unlike conformations. No assumption is made at this point of whether the AB interactions are stabilizing or destabilizing. The relationship of N_s to the individual constants for this example is given in eq 19.

$$(ES) = 2K_{AB}(1 + K_{AB})[K_sK_t(S)](A_4) \quad (20)$$

$$(ES_2) = K_{AB}(2K_{AB}^2 + 2K_{BB} + K_{AB} + K_{AB}K_{BB})[K_sK_t(S)]^2(A_4) \quad (21)$$

$$(ES_3) = 2K_{AB}K_{BB}(K_{AB} + K_{BB})[K_sK_t(S)]^3(A_4) \quad (22)$$

$$(ES_4) = K_{BB}^3[K_sK_t(S)]^4A_4) \quad (23)$$

$$N_s = \frac{2(K_{AB} + K_{AB}^2)[K_sK_t(S)] + 2(K_{AB}^2K_{BB} + 2K_{AB}^3 + K_{AB}^2 + 2K_{AB}K_{BB})[K_sK_t(S)]^2 + 6(K_{AB}^2K_{BB} + K_{AB}K_{BB}^2)[K_sK_t(S)]^3 + 4K_{BB}^3[K_sK_t(S)]^4}{1 + 2(K_{AB} + K_{AB}^2)[K_sK_t(S)] + (K_{AB}^2K_{BB} + 2K_{AB}^3 + K_{AB}^2 + 2K_{AB}K_{BB})[K_sK_t(S)]^2 + 2(K_{AB}^2K_{BB} + K_{AB}K_{BB}^2)[K_sK_t(S)]^3 + K_{BB}^3[K_sK_t(S)]^4} \quad (24)$$

"*Linear*" *Model.* In the linear case the two interior subunits react with each of two neighbors whereas the two terminal subunits react with only one neighbor. Therefore, the subunits can behave differently even though they may each have identical tertiary structure. The number of ways of binding S and the number of AB and BB pair interactions are given in Figure 3. The various species of ES complexes and the saturation equation are shown in eq 20–24.

"*Concerted*" *Model.* In the concerted model the conformations of all subunits change simultaneously. The various bindings of ligand to individual subunits are as shown in Figure 2. Since the subunit interactions all change concomitantly with the conformation change, only one constant, K_{tc}, is needed to encompass the equilibria previously allocated to K_t, K_{AB}, K_{BB}, etc. The concentrations of ES_i and the saturation equation similar to those shown above are given in eq 25–30. For this case, form B_4 with no S absorbed is included to make the equation analogous to previously derived equations (Monod *et al.*, 1965). This is in contrast to the derivations shown above in which conformation change for individual subunits occurred only when a molecule of ligand was bound. The saturation curve of eq 30 can be obtained from the equation derived by Monod *et al.* (1965) if it is assumed that only one of the two forms of the enzyme is capable of binding S.

$$(B_4) = K_{tc}^4(A_4) \quad (25)$$

$$(B_4S) = 4K_s(S)(B_4) \quad (26)$$

$$(B_4S_2) = 6K_s^2(S)^2(B_4) \quad (27)$$

$$(B_4S_3) = 4K_s^3(S)^3(B_4) \quad (28)$$

$$(B_4S_4) = K_s^4(S)^4(B_4) = K_s^4K_{tc}^4(A_4)(S)^4 \quad (29)$$

$$N_s = \frac{4K_s(S)[1 + K_s(S)]^3}{K_{tc}^{-4} + [1 + K_s(S)]^4} \quad (30)$$

Nonidentical Subunits. SQUARE CASE. In each of the above derivations it has been assumed that all subunits

are identical mathematically. By slight changes in the derivations alternative equations involving nonidentical subunits can be obtained. Because no new principles are involved and because a wide variety of possibilities makes the derivation of all the permutations of previously outlined cases extremely laborious, only some representative cases involving the square geometry will be elaborated.

A square case with two types of chains would behave as shown schematically in Figure 4. In this case α and β chains are arranged alternately and it is presumed, as discussed before, that diagonal interactions, *i.e.*, α–α, β–β, are excluded. This appears to be the case in hemoglobin (Perutz *et al.*, 1960).

Several possible alternatives still exist. For example, the two subunits may have different intrinsic binding constants. Equations 31 and 32 express these assumptions

$$K_{s\alpha} = \frac{(B_\alpha S)}{(B_\alpha)(S)} \tag{31}$$

$$K_{s\beta} = \frac{(B_\beta S)}{(B_\beta)(S)} \tag{32}$$

in which $K_{s\alpha}$ refers to the binding constant of the α chain and $K_{s\beta}$ to the β chain. Again, it is assumed that only the B conformation binds substrate. Another alternative is that the constant for the conformation change might be different, *i.e.*, $K_{t\alpha} \neq K_{t\beta}$.

For the case in which K_s varies and K_t is constant, eq 33, analogous to eq 18, arises. It is to be noted that the K_sK_t terms of eq 18 are now expanded to account for differences between the α and β chains, but that K_s and K_t always occur together. Thus, it is apparent that the form of this equation would be the same if K_s were held constant and two conformation constants $K_{t,\alpha}$ and $K_{t\beta}$ were substituted for K_t. In other words, the N_s dependence does not indicate whether the change occurs in K_s or K_t as the identity of the subunit changes. It is noted, of course, that both equations contain an additional constant so that more data would be needed to determine all the constants characterizing the saturation curve.

A second way in which nonidentical subunits might affect the saturation curve is by means of changed values for the interactions between subunits, either in K_{AB} or K_{BB} (*cf.* Figure 4). For example, the interactions along bracket 1 in Figure 4 are not necessarily the same as the interactions along bracket 2. Referring to the interaction along bracket 1′ in Figure 4 as $A_\alpha B_\beta$ and along bracket 2 as $A_\beta A_\alpha$ the two interaction constants could be characterized as $K_{A_\alpha B_\beta} \neq K_{B_\beta A_\alpha}$. This type of interaction can be considered pictorially as "rectangular" following a suggestion of Roughton *et al.* (1955). For such a case, assuming all K_{AB} values = 1, the concentrations of the various ES complexes are given by eq 34–37 and the saturation curve is given by eq 38.

Generalized Equation. Obviously, by altering the assumptions mentioned at the outset, many other variants of the saturation equations can be produced. It would not be fruitful to go through the derivation of all of them. One case is of sufficient interest to be mentioned here, using the square geometry as an illustrative example. If one assumes that the transformation A → B can take place even when no ligand S is bound to the subunit, a situation intermediate between the square case and the concerted transition is obtained. Several new forms of the enzyme–ligand complex can exist besides those listed in Figure 3, namely A_3B, A_2B_2, AB_3, B_4, A_2B_2S, AB_3S, B_4S, AB_3S_2, B_4S_2, and B_4S_3. By deriving expressions for the concentration of each species, eq 39 is obtained when $K_{AB} = 1$. By comparing this equation with eq 18, substituting $K_{AB} = 1$ in the latter, it can be seen that eq 39 can be obtained from eq 18 by factoring out $4K_s(S)$ from the numerator of the latter and then replacing $K_s(S)$ everywhere in the numerator and the denominator by

$$N_s = \frac{\begin{array}{r}2(K_{s\alpha}K_t + K_{s\beta}K_t)(S) + 2[(K_{s\alpha}K_t)^2 + (K_{s\beta}K_t)^2 + 4K_{BB}(K_{s\alpha}K_t)(K_{s\beta}K_t)](S)^2 + \\ 6K_{BB}^2(K_{s\alpha}K_t)(K_{s\beta}K_t)[K_{s\alpha}K_t + K_{s\beta}K_t](S)^3 + 4[(K_{s\alpha}K_t)(K_{s\beta}K_t)]^2K_{BB}^4(S)^4\end{array}}{\begin{array}{r}1 + 2(K_{s\alpha}K_t + K_{s\beta}K_t)(S) + [(K_{s\alpha}K_t)^2 + K_{s\beta}K_t)^2 + 4K_{BB}(K_{s\alpha}K_t)(K_{s\beta}K_t)](S)^2 + \\ 2K_{BB}^2(K_{s\alpha}K_t)(K_{s\beta}K_t)[(K_{s\alpha}K_t) + (K_{s\beta}K_t)](S)^3 + K_{BB}^4[(K_{s\alpha}K_t)(K_{s\beta}K_t)]^2(S)^4\end{array}} \tag{33}$$

$$(ES) = 4[K_sK_t(S)](A_4) \tag{34}$$

$$(ES_2) = 2(K_{B_\alpha B_\beta} + K_{B_\beta B_\alpha} + 1)[K_sK_t(S)]^2(A_4) \tag{35}$$

$$(ES_3) = 4K_{B_\alpha B_\beta}K_{B_\beta B_\alpha}[K_sK_t(S)]^3(A_4) \tag{36}$$

$$(ES_4) = K_{B_\alpha B_\beta}^2K_{B_\beta B_\alpha}^2[K_sK_t(S)]^4(A_4) \tag{37}$$

$$N_s = \frac{4[K_sK_t(S)] + 4(K_{B_\alpha B_\beta} + K_{B_\beta B_\alpha} + 1)[K_sK_t(S)]^2 + 12K_{B_\alpha B_\beta}K_{B_\beta B_\alpha}[K_sK_t(S)]^3 + 4K^2{}_{B_\alpha B_\beta}K_{B_\beta B_\alpha}{}^2[K_sK_t(S)]^4}{1 + 4[K_sK_t(S)] + 2(K_{B_\alpha B_\beta} + K_{B_\beta B_\alpha} + 1)[K_sK_t(S)]^2 + 3K_{B_\alpha B_\beta}K_{B_\beta B_\alpha}[K_sK_t(S)]^3 + K_{B_\alpha B_\beta}{}^2K_{B_\beta B_\alpha}{}^2[K_sK_t(S)]^4} \tag{38}$$

$$N_s = \frac{4K_tK_s(S) + 4K_t{}^2(1 + 2K_{BB})[1 + K_s(S)]K_s(S) + 12K_t{}^3K_{BB}{}^2[1 + K_s(S)]^2K_s(S) + 4K_t{}^4K_{BB}{}^4[1 + K_s(S)]^3K_s(S)}{1 + 4K_t[1 + K_s(S)] + 2K_t{}^2(1 + 2K_{BB})[1 + K_s(S)]^2 + 4K_t{}^3K_{BB}{}^2[1 + K_s(S)]^3 + K_t{}^4K_{BB}{}^4[1 + K_s(S)]^4} \tag{39}$$

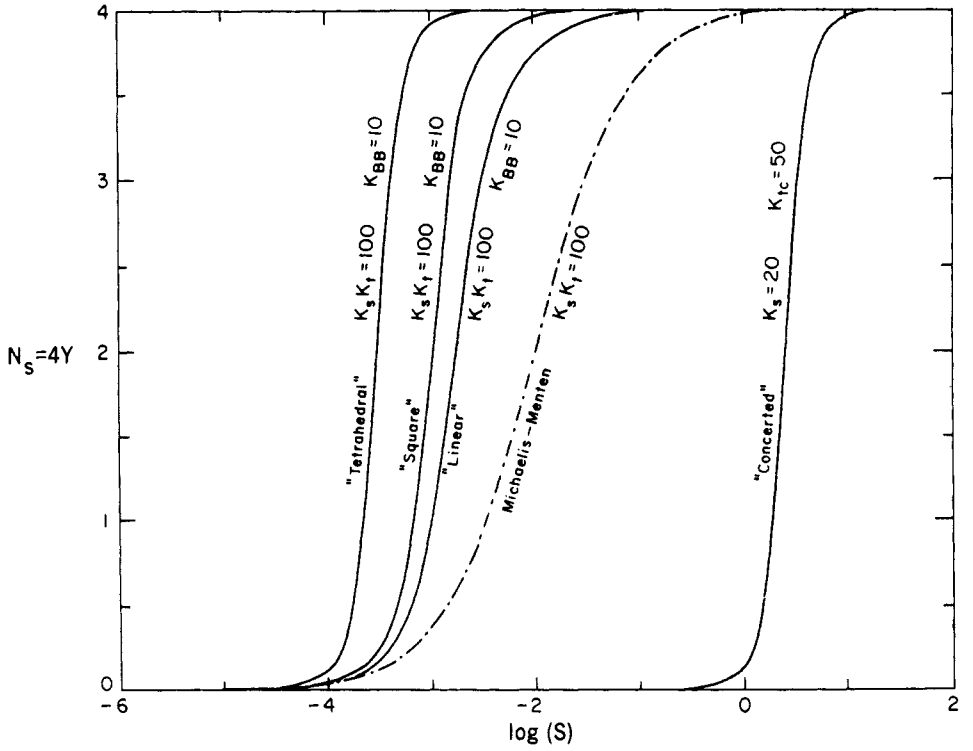

FIGURE 5: Examples of saturation curves for the various interaction geometries discussed in this paper and a comparison with a Michaelis–Menten curve (shown as —·—·—) having the same binding and transformation constants (K_s and K_t), but no subunit interactions ($K_{AB} = K_{BB} = 1$). $K_{AB} = 1$ for all curves. Constants for the concerted transition were chosen to give the same over-all constant for $A_4 + 4S \rightarrow B_4S_4$ as the square case (*cf.* discussion in text).

$1 + K_s(S)$. This is as expected, because for each form of the enzyme listed in Figure 3A, there are forms in which one or more BS units are replaced by B units, each such form giving rise to a new term in the equation for N_s.

Computation of Binding Curves. Binding curves giving N_s as a function of S were calculated and plotted using an IBM 7094 and a Calcomp digital computer plotting unit. Since it was desired to compare N_s using comparable coordinates over wide variation in S, N_s *vs.* log (S) plots were found to be more useful than N_s *vs.* (S) plots. In the log (S) plot more discrimination can be obtained at low concentrations of (S). In addition, the curves are easily tested for symmetry about the mid-point, and changes in the value of K_sK_t do not change the shape of the N_s–log (S) plots for the linear, tetrahedral, and square cases, making comparison of results easier.

Results

Effect of Changing Concentrations on Saturation Curves. Illustrative curves for the square, tetrahedral, linear, and concerted cases are shown in Figure 5. On comparing the curves with similar values for constants K_s and K_t and moderate interactions between B conformations, *i.e.*, $K_{BB} = 10$, it can be seen that the steepness of the curve increases as the total number of subunit interactions increases, *i.e.*, linear < square < tetrahedral. Moreover, the mid-point of the N_s–log (S) curve shifts to lower S concentrations, *i.e.*, for the same binding and conformation constants, less ligand concentration is required to half-saturate the enzyme.

The choice of constants for comparing the concerted mechanism with the others is less easy since the conformational change in the concerted case involves four subunits rather than 1. Therefore, numbers were chosen for K_s and K_{tc} in the concerted case to give the same value for the equilibrium constant of the over-all process, $A_4 + 4S = B_4S_4$, as in the square case shown in the same figure. By normalizing the two curves in this way it is seen that the concerted model curve is considerably steeper than the square case curve but the substrate concentration for half-saturation in the concerted model is much greater.

Although the different geometries give different saturation curves if the same intrinsic constants are chosen, the curves can be made to coincide closely by the proper selection of the various equilibrium constants. This is illustrated in Table I where values for N_s at different substrate concentrations are listed for the various models. The values do not coincide perfectly at all substrate concentrations, but accurate experimental data would be needed to distinguish even be-

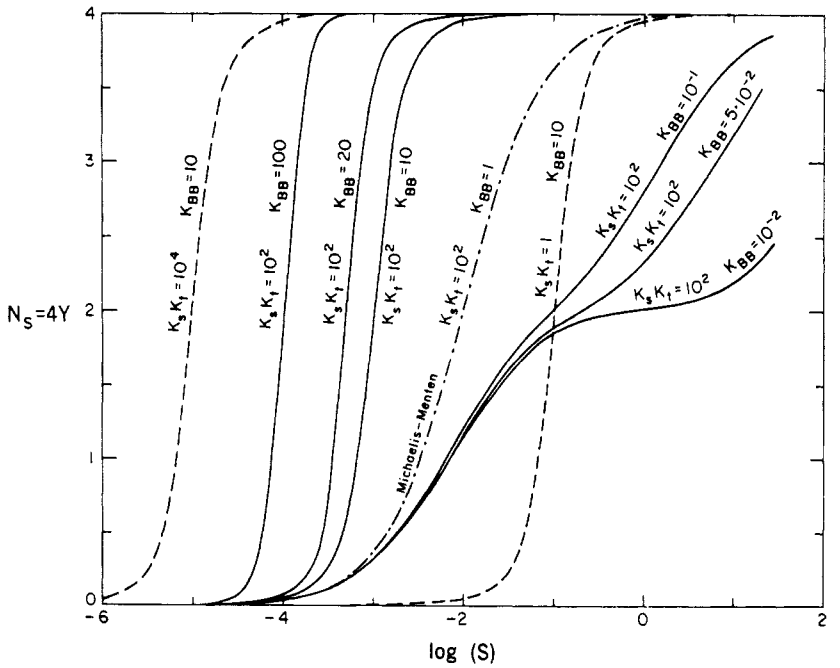

FIGURE 6: Examples of binding curves for the "square" geometry, showing the effect of changing K_sK_t (---------) or K_{BB} (———). K_{AB} = 1 for all curves. A Michaelis-Menten curve is shown (–·–·–·) for comparison.

TABLE I: Comparison of N_s Values at Several S Concentrations for Various Geometries when K_s, K_t, and K_{BB} Values Were Chosen by a Trial and Error Method in Order to Give Similar Curves.

	N_s Values			
(S)	Tetrahedral K_sK_t = 96 K_{BB} = 3	Square K_sK_t = 100 K_{BB} = 10	Linear K_sK_t = 100 K_{BB} = 20	Concerted K_s = 0.9 × 10^4 K_{tc} = 10^{-1}
10^{-4}	0.08	0.05	0.05	0.01
5×10^{-4}	0.72	0.57	0.68	0.30
9×10^{-4}	1.78	1.71	1.77	1.56
1×10^{-3}	2.00	2.00	2.00	2.00
2×10^{-3}	3.26	3.43	3.24	3.59
5×10^{-3}	3.79	3.88	3.77	3.90
10^{-2}	3.90	3.95	3.89	3.97

tween the cases selected by a trial and error method (*cf.* Table I). (Later the systematic fitting of curves will be discussed.)

It is to be noted that the assumptions that K_{AB} = 1 and K_{BB} = 1 for the square, linear, and tetrahedral cases are equivalent to the assumption that there is no net subunit interaction, *i.e.*, no net change in stability caused by the conformation change. These assumptions convert the saturation curves for the square, tetrahedral, and linear cases to the Michaelis–Menten equation. In the concerted model the assumption that $K_{tc} \gg 1$ will convert its saturation curve to the Michaelis–Menten equation also.

Effect of Changing the Various Equilibrium Constants on the Binding Curves. Although the trial and error method of fitting theory and experiment can be used, it was obviously desirable to obtain a less laborious method for this comparison. To do this it was first necessary to explore the effect of the individual equilibrium constants on the shape and (S) values of the saturation curves.

One immediate conclusion arises from the forms of the mathematical expressions. Except for eq 30 and 38, K_s and K_t always appear together as a product and, therefore, it will be impossible to obtain separate values of K_s or K_t by binding curves alone. Changing K_s or K_t together or separately shifts the binding curve along the substrate concentration axis without changing its shape (*cf.* Figure 6). In the concerted case, K_t and K_{BB} are not separable using only saturation data.

In Figure 6 some comparisons are given for various examples of the square case in which K_sK_t or K_{BB} are varied while K_{AB} is held constant. When K_{AB} = 1 and $K_{BB} > 1$, interactions between adjacent B conformations are more attractive than A–A interactions, whereas A–A and A–B interactions are equivalent. It is observed that increasing K_{BB} shifts ($S_{0.5}$) to lower values and tends to sharpen the transition, *i.e.*, decreases R_s.

When $K_{BB} < 1$ the curve tends to flatten at N_s = 2, and when $K_{BB} \ll 1$ it even may flatten for a very con-

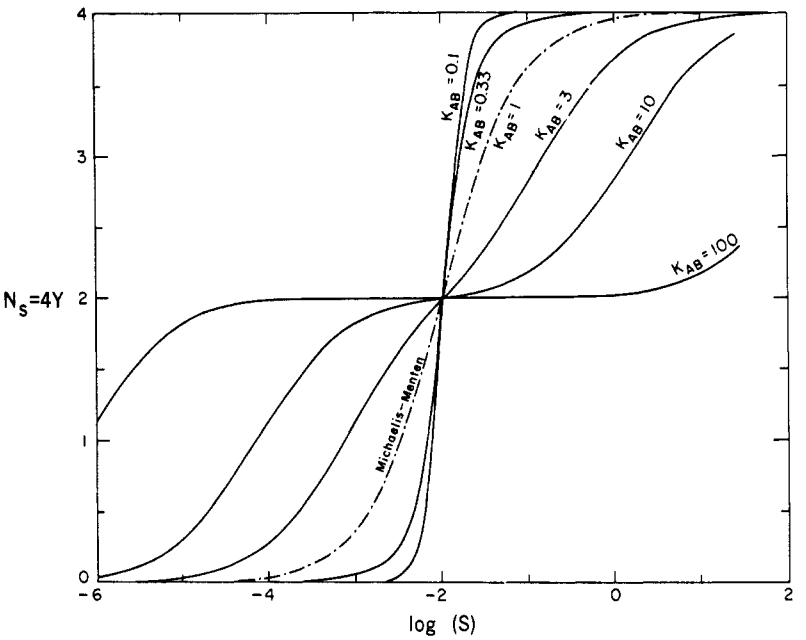

FIGURE 7: Examples of binding curves for the "square" geometry at constant K_{BB}, showing the effect of changing K_{AB}. $K_{BB} = 1$ and $K_sK_t = 10^2$ for all curves. A Michaelis–Menten curve is shown (–·–·–·) for comparison.

siderable range of substrate concentration. Thus, for a ligand of limited solubility, an experimental saturation curve of a protein containing four equivalent subunits with four equivalent binding sites might appear to indicate only two sites solely because K_{BB} is considerably less than 1.

In Figures 7 and 8 the effect of K_{AB} when K_{BB} and K_sK_t are held constant is seen. Since $K_{BB} = 1$ in Figure 7 the stabilities of AA and BB conformation are the same. If $K_{AB} > 1$ intermediate forms are stabilized relative to AA or BB, while if $K_{AB} < 1$ intermediate forms are relatively less stable. It is notable that all curves pass through the same value of $N_s = 2$ and that variations in K_{AB} tend to exert effects opposite to changes in K_{BB}. The latter observation can be pursued quantitatively, and it is found that for each choice of K_{BB} there is a value of K_{AB} which leads to a curve identical with the Michaelis–Menten curve. The relationship of constants required to satisfy this condition is given by eq 40.

$$K_{AB} = K_{BB}^{1/2} \tag{40}$$

which on substitution into eq 18 reduces the relationship to a Michaelis–Menten type expression (*cf.* eq 41).

$$N_s = \frac{4K_{BB}K_sK_t(S)}{1 + K_{BB}K_sK_t(S)} \tag{41}$$

Thus a Michaelis–Menten curve does not *per se* exclude the existence of interactions between subunits. The relationship of eq 40 can be generalized to any set of curves described by eq 18. For each family of curves which are identical in shape and merely differ in position along the abscissa, the two interaction constants are related by eq 42.

$$K_{AB} = cK_{BB}^{1/2} \tag{42}$$

In this equation, c can be obtained by selecting, from those curves for which $K_{AB} = 1$ (*cf.* Figure 7 or 9), the one coinciding best with the experimental curve. Then $c = 1/K_{BB}$ for this curve, and other combinations of K_{AB} and K_{BB} satisfying the experimental data can be obtained from eq 42. Using this relationship, the binding curve of eq 18 becomes eq 43.

$$N_s = \frac{4c^2K_{BB}^2[K_sK_t(S)] + 4(c^4K_{BB}^2 + 2c^2K_{BB}^2)[K_sK_t(S)]^2 + 12c^2K_{BB}^3[K_sK_t(S)]^3 + 4K_{BB}^4[K_sK_t(S)]^4}{1 + 4c^2K_{BB}[K_sK_t(S)] + 2(c^4K_{BB}^2 + 2c^2K_{BB}^2)[K_sK_t(S)]^2 + 4c^2K_{BB}^3[K_sK_t(S)]^3 + K_{BB}^4[K_sK_t(S)]^4} \tag{43}$$

It was found that eq 42 also applies to the tetrahedral case so that in that case also the family of curves can be reduced to a single set, corresponding to $K_{AB} = 1$. These relationships were helpful in developing the procedure outlined below.

Fitting Curves to Experimental Data. To test any model it is necessary to derive the theoretical curve which most closely approximates the data and compare it with the theoretical curves deduced from other models. When several models are to be tested and each model contains several independent parameters, curve

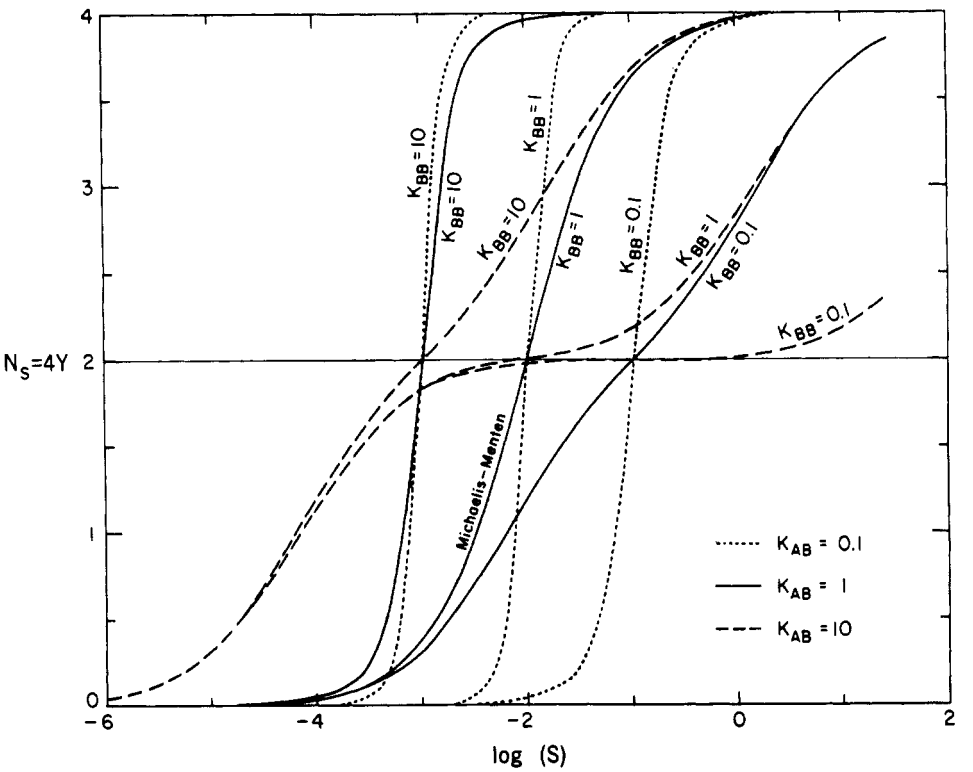

FIGURE 8: Examples of binding curves for the "square" geometry, showing the effect of varying both K_{AB} and K_{BB} simultaneously. $K_s K_t = 10^2$ for all curves. Curves with K_{AB} = constant are asymptotic at low (S), curves with the ratio K_{BB}/K_{AB} = constant are asymptotic at high (S), curves with K_{BB} = constant intersect at $N_s = 2.0$.

fitting by trial and error is excessively laborious. Although computers can be used and least-squares methods are available, these tools are inconvenient and expensive for routine use. Unless a more rapid method of curve fitting could be obtained, comparison of theory and experiment for more than one model would be prohibitive in time and money. Fortunately it was found that equations and nomograms could be devised which allow a choice of very good fits by the measurements of only three points on a sigmoid curve. The points selected were the substrate concentration at 50% of saturation, ($S_{0.5}$), and two points near the extremes of the saturation curve, *e.g.*, at 90 and 10% saturation. For convenience the latter two numbers are used as a ratio, R_s, since this ratio is also useful as an indication of the steepness of the curve.

Taketa and Pogell (1965) have used similar procedures to obtain nomograms for the n of the Hill equation. They found this parameter useful for characterizing the steepness of sigmoid curves and applied it to some characteristic enzyme data in the literature. Their procedure is valuable and the number n gives a convenient index of the steepness of the curve. However, since the models discussed here are more complex and do not follow the Hill equation, it was necessary to develop more detailed procedures for the more precise curve fitting required.

In Figure 9 log R_s' is plotted as a function of K_{BB} for the linear, square, and tetrahedral cases when $K_{AB} = 1$. In Figure 10 the relationship $-[\log K_s K_t + \log (S_{0.5})]$ is plotted *vs.* log K_{BB} for the same three geometric models.

From an experimental saturation curve the value of R_s is obtained. From Figure 9 the value of K_{BB} corresponding to this value of R_s is then read for each geometric model. The value of K_{BB} is used in Figure 10 to obtain the appropriate values for log $K_s K_t$ + log ($S_{0.5}$). From this number and the observed ($S_{0.5}$) the value of $K_s K_t$ is calculated. The last two steps can be simplified by the use of the nomogram in Figure 11. From the lines of Figure 10 it is clear that the data are related to each other by eq 44, where $\theta = 1$ for the square case,[1] 1.5 for the tetrahedral case, and ≈ 0.75 for the linear case. The significance of this relationship will be discussed in Appendix A.

$$\log (S_{0.5}) + \log K_s K_t = -\theta \log K_{BB} \qquad (44)$$

The nomograms are designed so they can be used with either R_s or R_s'. In some experimental situations the data may be limited to the 10–90% saturation range, in which case R_s would have to be used. In other cases, as will be discussed in the application to hemoglobin, both values may be useful. From the nomograms of Figure 11 either R_s or R_s' can be used to obtain the other constants of the theoretical model. In

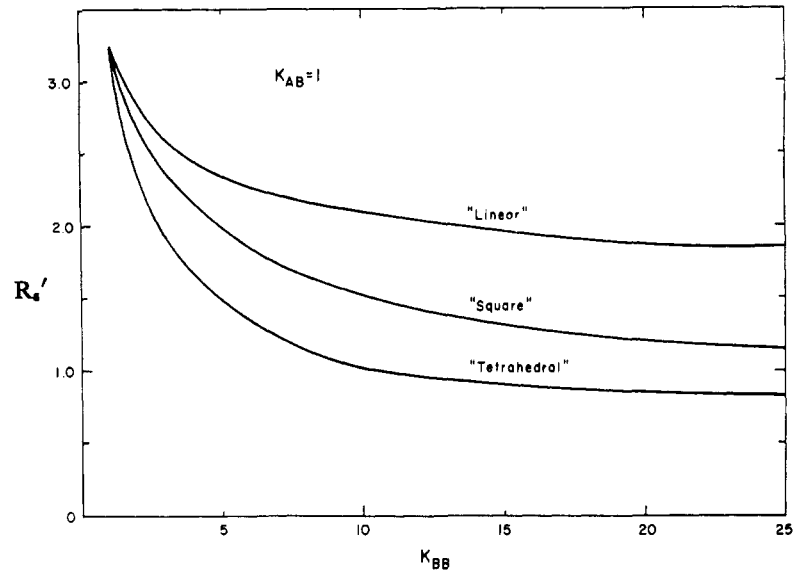

FIGURE 9: The parameter characterizing the sharpness of the transition of the saturation curve (R_s') as a function of K_{BB} for various geometries. If only R_s is known for a saturation curve instead of R_s', K_{BB} can be obtained from log R_s by first determining the corresponding value of log R_s' from one of Figures 11–13, and then using Figure 9 to determine K_{BB}.

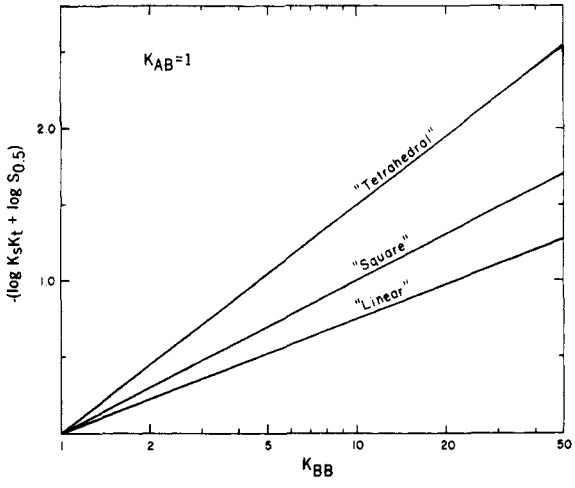

FIGURE 10: The quantity $-[\log K_s K_t + \log (S_{0.5})]$ as a function of K_{BB} for various geometries.

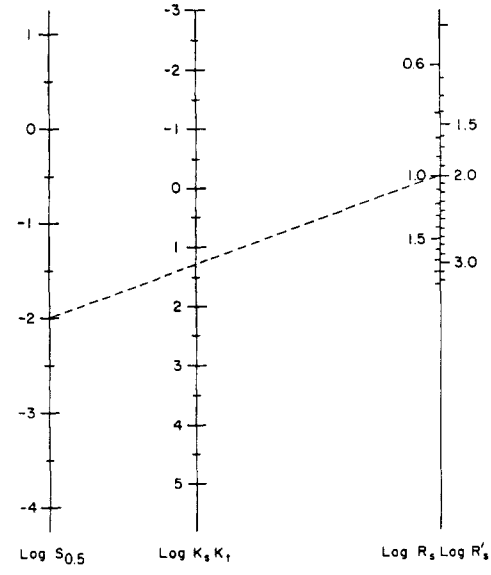

FIGURE 11: Nomogram for the "square" geometry, correlating $K_s K_t$ with the characteristic parameters of the saturation curve, ($S_{0.5}$) and R_s (or R_s') for K_{AB} = 1. The same nomogram can be used for curves characterized by either R_s or by R_s', by using the appropriate scale on the right-hand axis. The value of $K_s K_t$ applicable to a given saturation curve is obtained by connecting the appropriate log R_s and log ($S_{0.5}$) values by a straight line and reading the interaction of this line with the axis for log $K_s K_t$. For example, a saturation curve characterized by ($S_{0.5}$) = 10^{-2} and R_s = 10 corresponds to log $K_s K_t$ = 1.3, or $K_s K_t$ = 20, as shown by the dashed line.

Figures 9 and 10 only R_s' is listed as a function of K_{BB}. If R_s was obtained instead of R_s', the value of R_s' corresponding to R_s can be obtained from the nomogram, and this value can then be inserted into Figures 9 and 10 to obtain K_{BB}.

It is possible to use Figures 9–11 and 13 even if $K_{AB} \neq 1$ by using the relationship of eq 40 or 42. For a family of curves of known ($S_{0.5}$) the two interaction constants are obtained from eq 42 and c is obtained from Figure 9 or 10 as discussed above. When a pair of values for K_{AB} and K_{BB} is selected, $K_s K_t$ can be de-

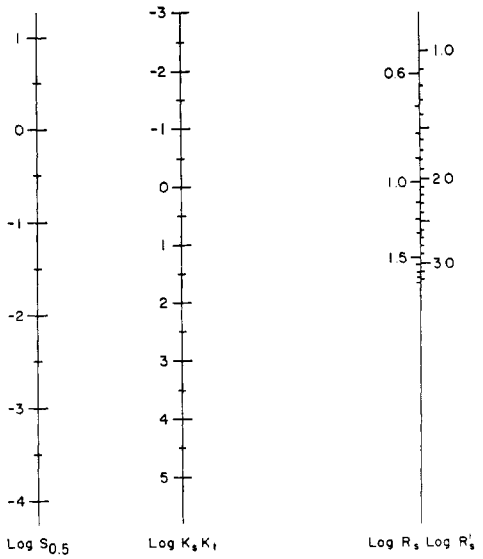

FIGURE 12: Nomogram for the "tetrahedral" geometry, correlating K_sK_t with the characteristic parameters of the saturation curve ($S_{0.5}$) and R_s (or R_s') for K_{AB} = 1. For use of the nomogram see the legend to Figure 11.

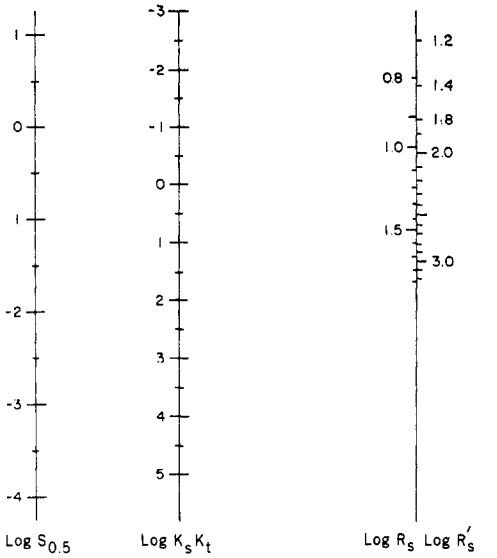

FIGURE 13: Nomogram for the "linear" geometry, correlating K_sK_t with the characteristic parameters of the saturation curve ($S_{0.5}$) and R_s (or R_s') for K_{AB} = 1. For use of the nomogram see the legend to Figure 11.

termined from Figure 10 or 11 since these plots are dependent only on K_{BB} and not on K_{AB} (*cf.* Figure 7).

In the case of other interaction geometries, *i.e.*, linear and tetrahedral, the same procedures can be followed. Corresponding curves are shown in Figures 9 and 10 and nomograms analogous to Figure 11 are shown in Figures 12 and 13.

If the subunits are not identical, the constants K_s and K_t may conceivably be split into four constants designated $K_{s\alpha}$, $K_{s\beta}$, $K_{t\alpha}$ and $K_{t\beta}$. For a given value of R_s and a selection of K_{BB}, the ratio of $K_{s\alpha}$ and $K_{s\beta}$ is fixed and *vice versa*. Figures 14 and 15 show the relationships of nonidentical subunits analogous to those previously shown in Figures 9 and 10 for identical subunits.

The parameter R_a or R_a' describing the degree of asymmetry of the curves can also be used in some cases to characterize saturation curves. However, it has been found that the curves for the square and tetrahedral cases are always symmetrical around the mid-point where $N_s = 2$ on the N_s–log (S) plot. The mathematical proof of this observation is outlined in Appendix B. In the linear case, the binding curve is asymmetrical, *i.e.*, $R_a \neq 1$, and increases with increasing values of K_{BB}.

The dependence of log R_s on K_{tc} for the concerted case is shown in Figure 16. The relationship between log ($S_{0.5}$) and the various constants is given in eq 45. The nomogram expressing the relationship of Figure 16 and eq 45 is given in Figure 17.

$$\log (S_{0.5}) + \log K_s = -\log K_{tc} \qquad (45)$$

Application to the O_2 Binding Data of Hemoglobin. As an illustration of the applicability of these procedures to experimental situations, the equations are applied to the O_2 binding data of hemoglobin. Since there are numerous binding studies of oxygen to hemoglobin and there are a number of different models, it was necessary to limit the number of applications and therefore four illustrative experimental situations were chosen. The first two were based on the data of Rossi-Fanelli *et al.* (1961) on human hemoglobin, at two different ionic strengths. They illustrate the changes in position and shape of the curves when ionic strength is varied. The third is taken from a study by Roughton *et al.* (1955) on sheep hemoglobin. The last is from the data of L. Lyster (quoted in Monod *et al.*, 1965) on horse hemoglobin which is quite similar to that of Rossi-Fanelli's.

Theoretical curves were obtained using the nomograms and procedures described above for each model, *i.e.*, square, tetrahedral, linear, and concerted. The only two parameters required to obtain the theoretical equations are R_s and ($S_{0.5}$) and the values of these two numbers which were used in the calculations are listed in Table II. To illustrate the type of fits obtained, a theoretical curve for each of the different models is shown in relation to the high ionic strength data of Rossi-Fanelli in Figure 18 and the fit of one theoretical model to all four sets of data are shown in Figure 19.

It is seen that the theoretical curve obtained from the square model agrees well with the high ionic strength study of Rossi-Fanelli *et al.* (1961). The same is true of the tetrahedral model whereas the linear and concerted models fit very poorly. As an aid in presenting the other data briefly, we shall give the square and tetrahedral curves from Figure 18 a rating of +++ to indicate a very good fit to the data, and the linear and concerted cases relative ratings of + to indicate a rather poor fit. In Table III a summary of the relative agreement be-

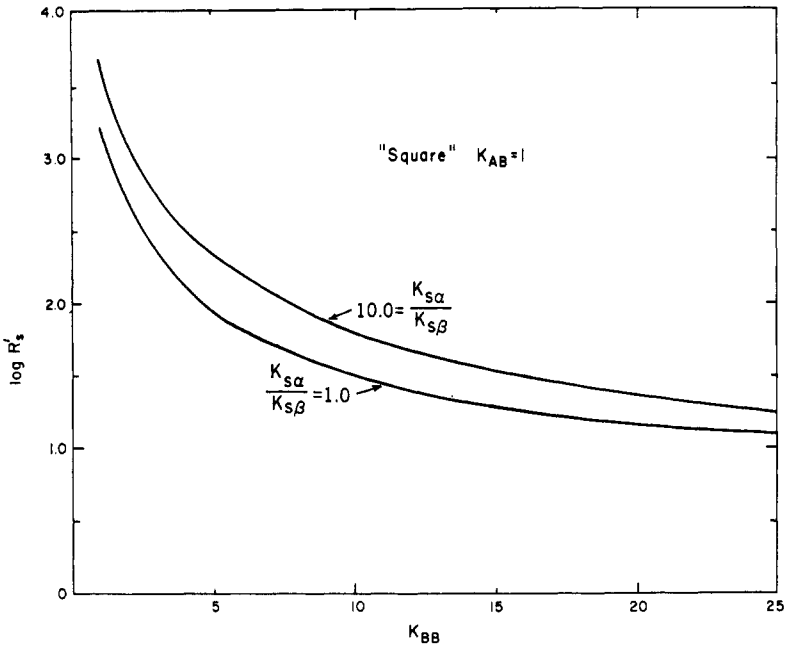

FIGURE 14: The parameter R_s as a function of K_{BB} for the "square" geometry with nonidentical subunits. In the case shown here, the binding constants $K_{s\alpha}$ and $K_{s\beta}$ are unequal. The labels on the curves indicate the value of the ratio $K_{s\alpha}/K_{s\beta}$. The ratio 1.0 corresponds to the square case treated before.

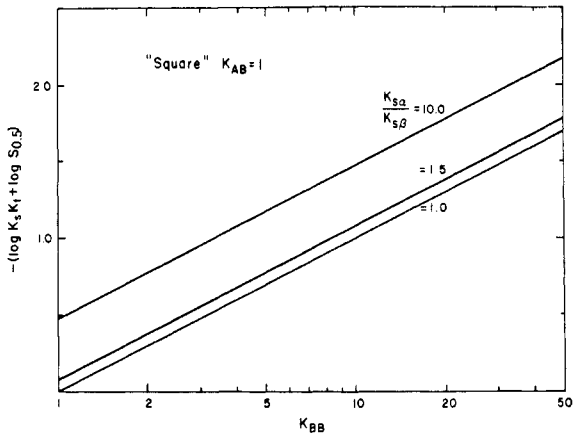

FIGURE 15: The quantity $-[\log K_s K_t + \log (S_{0.5})]$ as a function of K_{BB} for the "square" geometry with nonidentical subunits. Curves are shown for the case described in the legend of Figure 14.

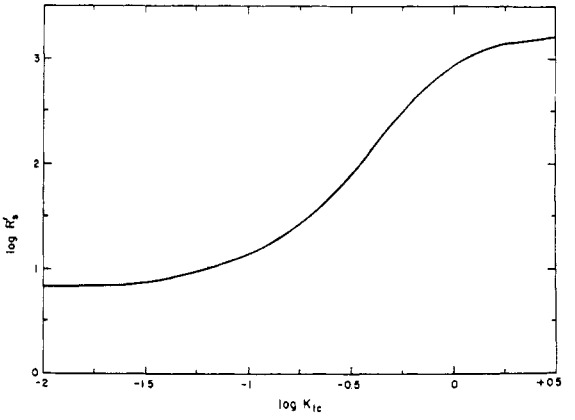

FIGURE 16: The parameter R_s' as a function of K_{tc} for the concerted transition case. If only R_s is available for a saturation curve, K_{BB} can be obtained with the aid of Figure 17 in the manner described in the legend of Figure 9.

tween theory and experiment for the different experimental situations is given. It is to be noted that the best fit for all four curves is obtained by the square model closely followed by the tetrahedral model. The linear and concerted cases are definitely poorer. The above fits were obtained using R_s' and $(S_{0.5})$. When the same process was repeated using R_s and $(S_{0.5})$ the results of Figure 20 and Table IV were obtained. It is to be noted that the square case now fits very well for all four sets of data, and the same is true for the tetrahedral model.

The linear and concerted models still give clearly less good representations of the experimental data. If the binding data were perfectly accurate and the models were completely correct, the same curve should obviously be obtained regardless of whether R_s or R_s' is utilized. This situation is essentially true for the square and tetrahedral models of curves B and C. In the case of curves A and D, *i.e.*, the low ionic strength curve of Rossi-Fanelli *et al.* (1961) and the data of L. Lyster

TABLE II: Characteristic Parameters of Hemoglobin Binding Curves.

Expt	Reference	Species	Experimental Conditions				Parameters of Binding Curve			
			t (°C)	pH	Buffer	Hb Concn	log R_s'	log R_s	log ($S_{0.5}$) (mm)	($S_{0.5}$) (mm)
A	Rossi-Fanelli *et al.*, 1961	Human	20	7.0	2.5×10^{-4} M phosphate	2×10^{-4} M	2.0	1.24	0.36	2.3
B	Rossi-Fanelli *et al.*, 1961	Human	20	7.0	2.5×10^{-1} M phosphate	2×10^{-4} M	1.4	0.70	0.96	9.1
C	Roughton *et al.*, 1955	Sheep	19	9.3	Borate	3–4%	1.26	0.67	0.63	4.3
D	Lyster (quoted in Monod *et al.*, 1965)	Horse	19	7	0.6 M phosphate	4.6%	1.78	0.74	1.00	10.0

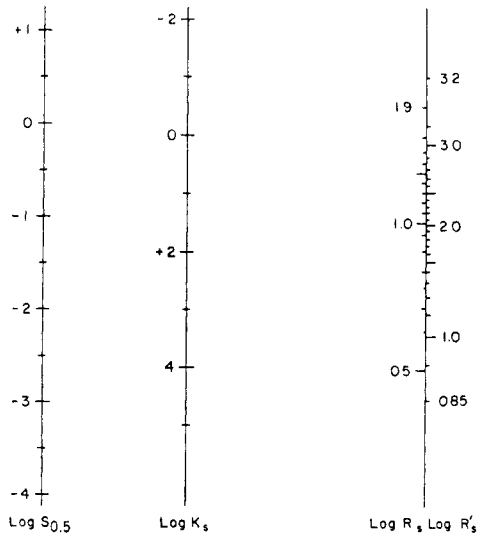

FIGURE 17: Nomogram for the concerted transition, correlating K_s with the characteristic parameters of the saturation curve, ($S_{0.5}$) and R_s (or R_s'). For use of the nomogram see the legend to Figure 11.

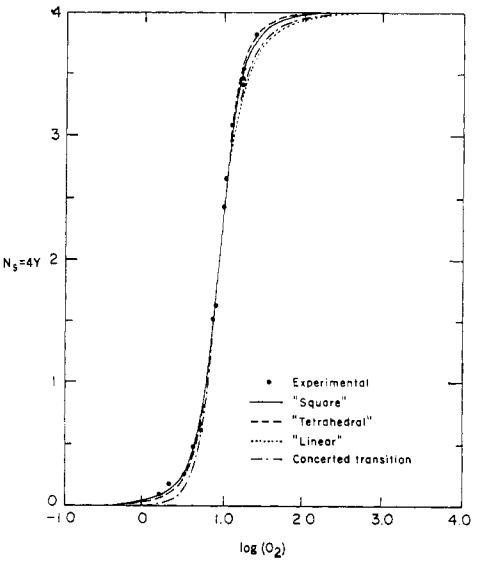

FIGURE 18: Comparison of the agreement between theory and experiment for various models and the oxygen binding data of hemoglobin. The parameters ($S_{0.5}$) and R_s' were used to fit the curves. The experimental points are taken from the data by Rossi-Fanelli *et al.* (1961) at high ionic strength. The line for the "square" geometry is identical with curve B of Figure 18. For the other geometries, the curves are drawn only where they do not coincide with the curve for the "square" case.

(quoted in Monod *et al.*, 1965), the fit of R_s is definitely better than with R_s'. Since the R_s' utilizes data at the extremes, *i.e.*, N_s = 3.9 and 0.1, whereas R_s utilizes data nearer the middle of the curve, *i.e.*, N_s = 3.6 and 0.4, this could mean that the data were less good at the extremes of binding for curves A and D. It could also, of course, mean that the models are not quite correct in these two cases. A choice between these two alternatives is not possible at the moment.

The Hill (1910) equation was tested only for a few examples but fit the data less well than the square and tetrahedral models. Although the theoretical curves were obtained in each case with the help of a computer, it is to be noted that the appropriate parameters in Table V were obtained simply from the nomograms and the two constants, ($S_{0.5}$) and either R_s or R_s'. Thus, it is relatively simple to test a given theoretical model, and a computer is helpful but certainly not necessary. A trial and error procedure becomes excessively laborious.

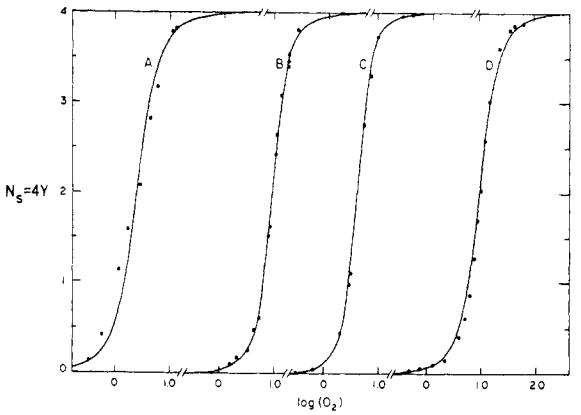

FIGURE 19: Application of the saturation equation for the "square" geometry (eq 18 with $K_{AB} = 1$) to the oxygen binding equilibrium of hemoglobin. Experimental points, taken from work by Rossi-Fanelli *et al.* (1961) at low ionic strength (A) and at high ionic strength (B), by Roughton *et al.* (1955) (C), and by Lyster (quoted in Monod *et al.*, 1965) (D) are shown by filled circles; the theoretical curves fitted to them are shown by full lines. The parameters ($S_{0.5}$) and R_s' ($= S_{0.975}/S_{0.025}$) used to fit the curves are listed in Table II. The equilibrium constants K_sK_t and K_{BB} for each curve are listed in Table V.

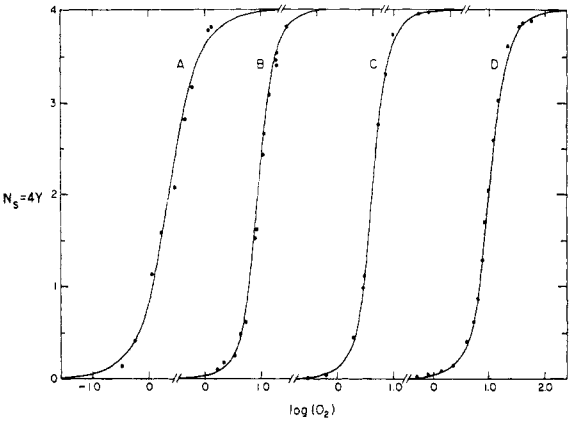

FIGURE 20: Application of the saturation equation for the "square" geometry to the oxygen binding equilibrium of hemoglobin. The parameters ($S_{0.5}$) and R_s ($= S_{0.9}/S_{0.1}$) were used to fit the curves. Otherwise, the data used are identical with those of Figure 18. The parameters used are listed in Table II, the equilibrium constants in Table V.

TABLE III: Relative Agreement of Theory and Experiment for "Linear," "Square," "Tetrahedral," and "Concerted" Models to Hemoglobin Saturation Curves Using R_s' and ($S_{0.5}$).[a]

	Relative Agreement on Scale of + to +++			
Exptl Curve	"Square"	"Tetrahedral"	"Linear"	"Concerted"
A	++	+	++	+
B	+++	+++	+	+
C	+++	+++	+	+
D	+++	+++	++	++

[a] Fitting procedure involved R_s' and ($S_{0.5}$) and the nomograms of Figures 11–13 and 17. Relative fit of curve to data based on Figure 18 as described in text, +++ being a very good fit, + being a curve that fits only part of the range.

TABLE IV: Relative Agreement of Theory and Experiment for "Linear," "Square," "Tetrahedral," and "Concerted" Models to Hemoglobin Saturation Curves Using R_s and ($S_{0.5}$).[a]

	Relative Agreement on Scale of + to +++			
Exptl Curve	"Square"	"Tetrahedral"	"Linear"	"Concerted"
A	+++	++	+++	+
B	+++	+++	++	+
C	+++	+++	+	++
D	+++	+++	++	++

[a] See Table III.

As illustrated above, it will frequently be desirable to pick additional points if agreement between theory and experiment is not good or if further confirmation of a given theoretical model is needed. Obviously, nomograms with other R_s values could be devised, *e.g.*, using $N_s = 3.0$ and 1.0. Whether added work required for such additional computation is desirable depends on the accuracy of the experimental data.

In Table V the numerical values for K_sK_t, etc., used to generate the curves giving the best fit for each of the models are given. It is to be noted that these numerical values differ widely for over-all curves that are very similar. Thus if it were possible to measure some of these parameters, for example, K_{BB}, independently, a final decision between the models which were indistinguishable on the basis of the saturation curve might emerge.

The allosteric model of Monod *et al.* (1965) fits the data of L. Lyster (quoted in Monod *et al.*, 1965) very well, whereas the concerted model fits it poorly. This may seem contradictory, since the concerted model is also based on the assumption of a simultaneous change in all subunit conformations. The reason for the difference is the extra parameter present in the allosteric model. There is no reason to add such a parameter to the square model since it fits the data already (*cf.*

TABLE V: Constants Characterizing the Theoretical Hemoglobin Binding Curves Giving the Best Fits to the Data.

Exptl Curve	"Square"		"Tetrahedral"		"Linear"		"Concerted"[a]	
	K_sK_t[b]	K_{BB}[c]	K_sK_t	K_{BB}	K_sK_t	K_{BB}	K_s	K_{tc}
			Based on R_s' [= ($S_{0.975}/S_{0.025}$)] and ($S_{0.5}$)					
A	8.7×10^{-2}	5.0	9.3×10^{-2}	2.8	6.5×10^{-2}	13.0	1.24	0.35
B	8.8×10^{-3}	12.5	8.3×10^{-3}	5.6	5.8×10^{-3}	50.0	0.65	0.17
C	1.3×10^{-2}	17.4	1.3×10^{-2}	6.8	6.5×10^{-3}	120.0	1.90	0.63
D	1.5×10^{-2}	6.7	1.6×10^{-2}	3.5	8.9×10^{-3}	25.0	0.36	0.28
			Based on R_s [= ($S_{0.9}/S_{0.1}$)] and ($S_{0.5}$)					
A	1.47×10^{-1}	2.9	1.86×10^{-1}	1.8	1.20×10^{-1}	5.5	0.95	0.52
B	8.1×10^{-3}	13.5	7.3×10^{-3}	6.1	2.6×10^{-3}	150.0	0.63	0.17
C	1.6×10^{-2}	14.8	1.3×10^{-2}	6.7	2.2×10^{-3}	500.0	1.60	0.15
D	9.3×10^{-3}	10.7	8.3×10^{-3}	5.2	2.8×10^{-3}	116.0	0.50	0.20

[a] Concerted case: [K_s] = mm^{-1}; K_{tc} = dimensionless. [b] K_sK_t has dimensions of mm^{-1}. [c] K_{BB} is dimensionless.

Figure 21). The fact that the concerted model requires an extra parameter to give agreement does not, however, *a priori* mean that it is incorrect. The number of parameters and the accuracy of models are discussed below.

Discussion

The mathematical relationships to a certain extent speak for themselves. Some qualitative conclusions, however, which are drawn from these saturation curves and their application to a specific curve perhaps deserve emphasis.

1. Evidence for a Given Mechanism from a Saturation Curve. Although it is quite clear that accurate experimental data can in certain cases distinguish between the various models, it is also evident that different constants can be chosen for each geometry; these constants are capable of giving very similar curves. In many cases the points which deviate significantly from each other are at the extremes of ligand concentration where the experimental data may be most difficult to obtain. Furthermore, it is seen that wide variation in the steepness of curves, their point of half-saturation, their binding constants, etc., can be obtained with rather simple models containing a minimum of arbitrary parameters, *i.e.*, without assuming nonidentical subunits or differences in the orientation of one subunit to another. For example, in the case of hemoglobin a fit to the experimental data which is within experimental error can be obtained by more than one model of subunit interactions involving rather wide variations in intrinsic constants. It seems probable, therefore, that saturation curves *per se* will not be capable of establishing unique mechanisms.

Furthermore, it seems clear that even given a single, unique mechanism it will be frequently impossible to obtain unambiguous values for individual constants. Thus K_s and K_t appear together as products in many of the expressions and, therefore, it would be impossible to obtain specific values for these constants even if the data were perfectly accurate. Similarly, only the ratio of K_{AB} to $K_{BB}^{1/2}$ can be obtained because the saturation curves have the same shape for a constant value of this ratio.

The accuracy of the fit between experimental data and theoretical model is always made easier by increasing the number of arbitrary parameters. In some cases these added parameters arise of necessity, *e.g.*, to allow for known differences in subunits, but each added parameter included in the expression requires that alternative models with equivalent numbers of adjustable parameters be tested. Thus if the fit to the experimental data demands additional parameters, the probability that a unique mechanism can be established by a saturation curve decreases.

2. Distinguishing Mechanisms by Alternative Sources of Information. The fact that a saturation curve *per se* does not indicate a unique mechanism does not mean that no information is obtained. It is clear that the square and tetrahedral models described above fit the data far better than the linear and concerted models. If the deviations in the latter cases are outside experimental error, these mechanisms as outlined in eq 24 and 30 can be excluded.

If several models give curves which fit the data, further information will be necessary to obtain a unique mechanism. Table V gives an indication of the type of data which may be helpful in this regard. For example, the experimental points in A can be fitted by curves which are very similar, derived from the four different models presented above. However, the K_sK_t values which are required to give these similar curves are 8.7×10^{-2}, 9.3×10^{-2}, and 6.5×10^{-2}, respectively. The respective K_{BB} values are 5.0, 2.8, and 13.0. Clearly an independent method of measuring K_sK_t or K_{BB} could distinguish between these alternatives. Although no method of measuring precisely these quantities exists at the moment, these calculations indicate lines which may lead to such distinctions.

Optical rotatory dispersion spectra, difference spec-

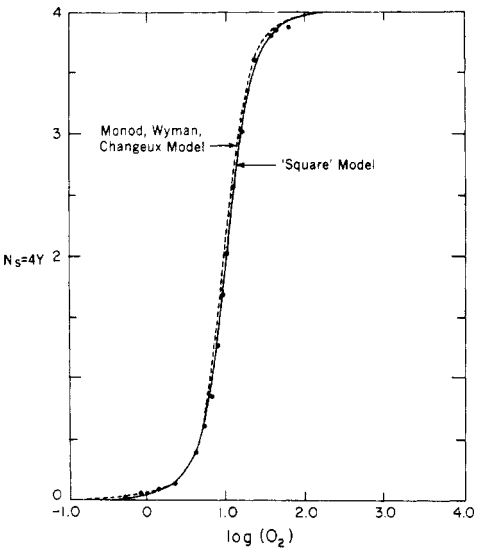

FIGURE 21: Comparison of the use of the equation for the "square" geometry (———) and the equation derived by Monod *et al.* (1965) (---------) in fitting the data for the oxygen binding equilibrium of hemoglobin. The experimental points are taken from the data of L. Lyster (quoted in Monod *et al.*, 1965). The curve for the "square" case was adjusted by using the parameters ($S_{0.5}$) and R_s and is identical with curve D of Figure 20. The curve for the equation of Monod *et al.* (1965) was redrawn from the figure presented by them, using the values of the constants shown in that curve, *i.e.*, $L = 9054$, $c = 0.014$, and $K_R = 1.0$, the latter being determined directly from the curve shown by them.

tra, etc., may provide information in this regard. Correlation of binding constants with observed conformational changes, for example, would provide an extra source of information. Moreover, the three-dimensional geometry of the protein as determined by X-ray crystallography may be helpful in eliminating alternatives. For example, in the case of hemoglobin the subunits appear to be arranged in a roughly tetrahedral arrangement, but there are apparently few diagonal interactions. Thus the square case outlined above would appear to be preferable to the tetrahedral model as judged by the three-dimensional arrangement of the molecule. The finding that monomeric myoglobin gives a curve consistent with the Michaelis–Menten equation suggests that the interaction parameters K_{AB} and K_{BB} are indeed responsible for the changed saturation curve in hemoglobin (Theorell, 1934; Rossi-Fanelli *et al.*, 1964). Finally, the fit of a single model to saturation curves obtained under a wide variety of conditions might be helpful. For example, the fact that the square case gives good agreement with the experimental saturation curves is indicative that it may be a correct representation of the molecule. Thus, saturation curves *per se* may not distinguish but they may so limit the alternatives that even moderately accurate additional measurements may allow a unique representation of the data. Perhaps one of the most valuable results of these equations is to indicate the types of measurements which may be useful.

3. Qualitative Conclusions from Saturation Curves. The difficulty of direct measurement of conformational effects makes it desirable to derive qualitative conclusions from saturation curves, but this procedure has its perils. Thus, it is frequently assumed that a Michaelis–Menten type curve indicates the absence of cooperative effects or of subunit interactions. Actually, as shown here, subunit interactions may occur and still give a Michaelis–Menten curve. To do so requires certain quantitative limitations which may be rare. However, the probability of these occurrences is not yet known. Hence, the existence of a Michaelis–Menten curve can be considered as an indication of the absence of cooperative or antagonistic effects but certainly not as conclusive evidence in this regard.

Another interesting relationship is the finding that a saturation curve when $K_{AB} \gg 1$ or $K_{BB} \ll 1$ levels out at $Y = 0.5$ over a wide range of ligand concentrations. This would mean that four identical subunits with four identical sites can give the appearance of two sites as a result of subunit interactions. Other assumptions in K values could likewise give rise to similar anomalies.

Finally, it is worth emphasizing that a curve with a very steep rise and a classical sigmoid pattern can be obtained equally well when $K_{BB} = 1$ and $K_{AB} < 1$ as when $K_{AB} = 1$ and $K_{BB} > 1$. Thus the appearance of such a sigmoid curve is not a necessary indication that there is a cooperative effect between subunits to stabilize a conformational change. Rather an unfavorable interaction between identical subunits in different conformations might have the same effect.

4. Nonidentical Subunits. The presence of subunits of differing amino acid sequence may influence the constants of the system, but such an influence is not a necessity. If the amino acid differences occur in nonessential parts of the molecule no perturbations of ligand binding or subunit interactions may occur. There are examples of enzymes from different species having different amino acid sequences which have apparently identical catalytic activities (Smith and Margoliash, 1964). Thus the difference between the α and β chains of hemoglobin does not *a priori* indicate that their binding sites are different or that their interaction with each other is necessarily different. The presence of different types of chains, therefore, allows an added parameter which may or may not be important in the systems under investigation.

Since there is strong evidence that primary sequence determines tertiary structure it can be presumed that subunits of identical amino acid sequence have the same tertiary structure, and, therefore, presumably the same interactions.

5. Fitting of Curves to Data. The empirical curve-fitting procedure outlined above was designed for simplicity and relative accuracy for the class of proteins which are being intensively investigated at the

moment. The fit obtained in the hemoglobin case was within experimental error of the O_2 binding data. It seems wasteful to obtain the very best fit by elaborate least-squares methods for a given model when several different models are capable of explaining the data. At this stage, therefore, further methods of refinement did not seem worth developing. However, as the data become more accurate and the need to distinguish between mechanisms more urgent, the procedures outlined here could readily be extended. It should be emphasized, however, that possible developments of the future might go in an entirely different direction. Thus the development of independent methods of measuring K_s and K_t might make it superfluous to obtain highly accurate saturation curves in order to distinguish between mechanisms.

In applying these models to other experimental situations it is important to caution against blind use of the nomograms provided here. For a four-subunit enzyme the nomograms may be helpful and a fit of theory and experiment may indicate the mechanism or mechanisms worthy of further consideration. Until all likely other alternatives are excluded, however, a fit does not establish an individual model.

In applying such procedures to other systems, *e.g.*, those involving more or less than four subunits, the procedures used here are readily applied. A model similar to those in Figure 2 must be prepared. The detailed relationships as depicted in Figure 3 must be outlined. From these the derivations are relatively easy, the coefficients of the terms being closely related to the numbers found in Figure 3. Thus, although the equations look formidable, they can be derived and computed with relative ease by the procedures utilized for these tetramer cases.

Using a family of ligand curves such as those in Figures 6–8, it is easy to construct nomograms for R_s ratios other than those used here. This might be desirable in certain situations, *e.g.*, when a given protein could only be studied between 75 and 25% saturation.

6. Catalyzed Transformation vs. Tautomerism. In a ligand-induced conformation change two mechanisms of achieving the end result may be visualized. One is a catalyzed transformation in which the substrate accelerates the rate of the conformation change. The other is tautomerism in which the protein by itself undergoes the conformation change and the new form is then subsequently complexed by the ligand. Both alternatives can be stated in the form of eq 46 in which the relative velocities of pathway 3 *vs.* pathway 1 plus 2 will determine the mechanism of the conformation change.

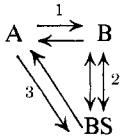

(46)

In the derivations of this paper no attempt to distinguish between these alternatives was made. A model containing BS forms but not B forms tacitly assumes that no significant quantities of B exist in the absence of S. Whether this occurs because of kinetics or equilibrium is a significant problem, but it does not need to be resolved for the present work and, therefore, it is not examined in this paper.

7. Relation of Models to the Actual Conformational Changes in the Protein. The fact that a good fit to hemoglobin data was obtained with rather simple models does not mean that these simple models are necessarily correct. It does mean, however, that the saturation curves *per se* do not demand at this stage of study more complex models. For example, the square model shown above fits the hemoglobin data very well. This model involved assumptions that: (a) only two conformations, A and B, exist; (b) that there are strong interactions between adjacent B conformations; and (c) that the interactions between the adjacent A conformations is the same as between adjacent A–B conformations. From what we know of protein chemistry these assumptions do not seem likely to be rigorously true in all cases. It is difficult to believe that a change which makes B very strongly interact with another B will leave unchanged its interaction with A. Moreover, a partial change in the A conformation might be caused by a change in an adjacent B structure, thus giving a conformation intermediate between A and B. These relations could be expressed mathematically, and one such intermediate case was calculated in this article. It was obviously undesirable, however, to calculate all the intermediate situations when the more extreme models already fit the data. Moreover, the added complexities may be minor perturbations on a basic model which may be close to that of one of the simple cases outlined here.

Only future experiments can distinguish between the alternatives, but the mathematical identification of individual constants and detailed fitting of saturation curves appear to provide one avenue for obtaining such distinctions.

Appendix A

Relationship of the Half-Saturation Point ($S_{0.5}$) to the Equilibrium Constants. (*1*) DEPENDENCE ON K_{BB}. Only $K_{AB} = 1$ will be considered in this section, since ($S_{0.5}$) is independent of the value of K_{AB} (*cf.* section 2 below and Figure 7).

Equation 44 can be rewritten as

$$K_{BB}^{\theta} K_s K_t (S_{0.5}) = 1 \qquad \text{(A1)}$$

The validity of this relationship will be verified in this section. By raising both sides of eq A1 to the nth power ($n = 4$ in this case) and comparing with eq 12, 17, and 23, it can be seen that eq A1 is equivalent to the condition

$$\frac{(ES_4)}{(ES_0)} = \frac{(B_4S_4)}{(A_4)} = 1 \qquad \text{(A2)}$$

for the tetrahedral, square, and linear cases, respectively. For example, if eq A1 holds, then for the square case

$$\frac{(ES_4)}{(A_4)} = K_{BB}^4(K_sK_t)^4(S)^4 = 1 \qquad (A3)$$

and similarly for the other cases. Using eq 29 and 45 in the same manner, it can be seen that eq A2 is also obeyed for the concerted transition.

By using eq 9 and 11, or 14 and 16, respectively, it can also be seen that eq A1 implies that

$$\frac{(ES_3)}{(ES)} = \frac{(AB_3S_3)}{(A_3BS)} = 1 \qquad (A4)$$

for the square and the tetrahedral cases.

For example, for the square case,

$$\frac{(ES_3)}{(ES)} = \frac{4K_{BB}^2(K_sK_t)^3(S)^3}{4K_sK_t(S)}$$

$$= K_{BB}^2(K_sK_t)^2(S)^2 = 1 \qquad (A5)$$

Equations A2 and A4 imply that, when eq A1 is satisfied, then the distribution of E in the various forms ES_i (i = 0–4) is symmetrical with respect to ES_2. Therefore, the amount of substrate bound can be written as

$$\sum_{i=0}^{4} i(ES_i) = 0(ES_0) + (ES_1) + 2(ES_2) + 3(ES_1) +$$

$$4(ES_0) = 4(ES_1) + 2(ES_2) + 4(ES_0) \qquad (A6)$$

while the amount of enzyme is given by

$$\sum_{i=0}^{4} (ES_i) = (ES_0) + (ES_1) + (ES_2) +$$

$$(ES_1) + (ES_0) = 2(ES_1) + (ES_2) + 2(ES_0) \qquad (A7)$$

Substituting eq A6 and A7 into eq 5 gives N_s = 2, verifying that eq A1 represents the condition for the mid-point for the square and the tetrahedral curves.

The relationship A4 does not hold for the linear case, due to the asymmetry of the saturation curve (*cf.* Appendix B). Using eq 20 and 22, it can be seen that

$$\frac{(ES_3)}{(ES)} = K_{BB}\frac{1 + K_{BB}}{2}(K_sK_t)^2(S)^2 \qquad (A8)$$

instead of

$$K_{BB}^{1.5}(K_sK_t)^2(S)^2$$

which would be required if eq A1 and A4 were to hold.

Therefore, the condition given in the text for the mid-point of the linear curve, *i.e.*, eq 44 with θ = 0.75, is only an approximation.

(2) Dependence on K_{AB}. As shown in Figures 7 and 8 for the square case, the mid-points of all curves with constant values of K_sK_t and of K_{BB} coincide, irrespective of the choice of K_{AB}. This relationship holds for the tetrahedral case as well.

As seen from eq 9 and 11, or 14 and 16, respectively, the number of A–B interactions is the same in the forms ES and ES_3 in both cases. Therefore, if $K_{AB} \neq 1$, both (ES_1) and (ES_3) contain the same factor, K_{AB}^3 (or K_{AB}^2) and eq B4 still holds. In other words, the symmetry of the distribution of E (eq A6 and A7) is not altered by changing K_{AB}.

Appendix B

Symmetry of Saturation Curves. Symmetry of the saturation curve in the N_s *vs.* log (S) representation requires that $R_a = R_a' = 1$, with a similar relationship holding for all similar choices of two points equidistant from N_s = 2.0. From eq 7 this condition can be expressed as

$$\frac{(S_{0.5+x})}{(S_{0.5})} = \frac{S_{(0.5)}}{(S_{0.5-x})} = \lambda \qquad (B1)$$

where λ is substituted for the ratio shown in order to simplify the expressions to be derived. With this substitution,

$$(S_{0.5+x}) = (S_{0.5})\lambda \qquad (B2)$$

and

$$(S_{0.5-x}) = (S_{0.5})/\lambda \qquad (B3)$$

From eq 44 it can be seen that

$$K_sK_t(S_{0.5}) = K_{BB}^{-\theta} \qquad (B4)$$

Using this relationship with eq B2 and B3,

$$K_sK_t(S_{0.5+x}) = \frac{\lambda}{K_{BB}^{\theta}} \qquad (B5)$$

and

$$K_sK_t(S_{0.5-x}) = \frac{1}{\lambda K_{BB}^{\theta}} \qquad (B6)$$

In the following, only saturation curves for which K_{AB} = 1 will be discussed, in order to simplify the equations. However, the present proof can easily be extended to $K_{AB} \neq 1$ using the relationship shown in eq 41.

For the square case, for which θ = 1, substitution of (S_I) = ($S_{0.5+x}$) and of (S_{II}) = ($S_{0.5-x}$) in eq 18 gives, respectively

$$N_{sI} = \frac{4K_{BB}^{-1}\lambda + 2(2K_{BB} + 1)K_{BB}^{-2}\lambda^2 + 12K_{BB}^{-1}\lambda^3 + \lambda^4}{1 + 4K_{BB}^{-1}\lambda + 2(2K_{BB} + 1)K_{BB}^{-2}\lambda^2 + 4K_{BB}^{-1}\lambda^3 + \lambda^4} \tag{B7}$$

and

$$N_{sII} = \frac{4K_{BB}^{-1}\lambda^{-1} + 2(2K_{BB} + 1)K_{BB}^{-2}\lambda^{-2} + 12K_{BB}^{-1}\lambda^{-3} + 4\lambda^{-4}}{1 + 4K_{BB}^{-1}\lambda^{-1} + (2K_{BB} + 1)K_{BB}^{-2}\lambda^{-2} + 4K_{BB}^{-1}\lambda^{-3} + \lambda^{-4}} \tag{B8}$$

Multiplying numerator and denominator on the right-hand side of eq B8 by λ^4 and adding it to eq B7 gives

$$N_{sI} + N_{sII} = \frac{4 + 16K_{BB}^{-1}\lambda + 4(2K_{BB} + 1)K_{BB}^{-2}\lambda^2 + 16K_{BB}\lambda^3 + 4\lambda^4}{1 + 4K_{BB}^{-1}\lambda + (2K_{BB} + 1)K_{BB}^{-2}\lambda^2 + 4K_{BB}\lambda^{-3} + \lambda^4} = 4 \tag{B9}$$

By definition,

$$N_{sI} + N_{sII} = (2.0 + x) + (2.0 - x) = 4.0 \tag{B10}$$

Because the equality of eq B9 and B10 hold independently of the choice of either x or K_{BB}, it can be seen that all curves for the square case are symmetrical. By a similar argument, it can be shown that all tetrahedral curves must be symmetrical, too.

In the linear case, for which $\theta = 0.75$, the same procedure gives, in place of eq B7–B9, the following expressions based on eq 24.

$$N_{sI} = \frac{4K_{BB}^{-0.75}\lambda + 6(1 + K_{BB})K_{BB}^{-1.5}\lambda^2 + 6(1 + K_{BB})K_{BB}^{-1.25}\lambda^3 + 4\lambda^4}{1 + 4K_{BB}^{-0.75}\lambda + 3(1 + K_{BB})K_{BB}^{-1.5}\lambda^2 + 2(1 + K_{BB})K_{BB}^{-1.25}\lambda^3 + \lambda^4} \tag{B11}$$

and

$$N_{sII} = \frac{4K_{BB}^{-0.75}\lambda^{-1} + 6(1 + K_{BB})K_{BB}^{-1.5}\lambda^{-2} + 6(1 + K_{BB})K_{BB}^{-1.25}\lambda^{-3} + 4\lambda^{-4}}{1 + 4K_{BB}^{-0.75}\lambda^{-1} + 3(1 + K_{BB})K_{BB}^{-1.5}\lambda^{-2} + 2(1 + K_{BB})K_{BB}^{-1.25}\lambda^{-3} + \lambda^{-4}}$$

$$= \frac{4K_{BB}^{-0.75}\lambda^3 + 6(1 + K_{BB})K_{BB}^{-1.5}\lambda^2 + 6(1 + K_{BB})K_{BB}^{-1.25}\lambda + 4}{1 + 2(1 + K_{BB})K_{BB}^{-1.25}\lambda + 3(1 + K_{BB})K_{BB}^{-1.5}\lambda^2 + 4K_{BB}^{-0.25}\lambda^3 + \lambda^4} \tag{B12}$$

Adding eq B11 and B12, it can be seen that the expressions containing K_{BB} do not vanish from the sum as they do in eq B9, except in a few special cases, *i.e.*, R_a is a function of K_{BB}, and that, therefore, the linear case does not result in symmetrical saturation curves.

References

Adair, G. S. (1925), *J. Biol. Chem. 63*, 529; *Proc. Roy. Soc. (London) A109*, 292.

Atkinson, D. E., Hathaway, J. A., and Smith, E. C. (1965), *J. Biol. Chem. 240*, 2682.

Atkinson, D. E., and Walton, G. M. (1965), *J. Biol. Chem. 240*, 757.

Coryell, C. D. (1939), *J. Phys. Chem. 43*, 841.

Gerhart, J. C., and Pardee, A. B. (1962), *J. Biol. Chem. 237*, 891.

Grisolia, S. (1964), *Physiol. Rev. 44*, 657.

Hill, A. V. (1910), *J. Physiol. (London) 40*, 190.

Koshland, D. E., Jr. (1963), *Science 142*, 1533.

Koshland, D. E., Jr., Yankeelov, J. A., Jr., and Thoma, J. A. (1962), *Federation Proc. 21*, 1031.

Michaelis, L., and Menten, M. (1913), *Biochem. Z. 49*, 333.

Monod, J., Changeux, J.-P., and Jacob, F. (1963), *J. Mol. Biol. 6*, 306.

Monod, J., Wyman, J., and Changeux, J.-P. (1965), *J. Mol. Biol. 12*, 88.

Pauling, L. (1935), *Proc. Natl. Acad. Sci. U. S. 21*, 186.

Perutz, M. F., Bolton, W., Diamond, R., Muirhead, H., and Watson, H. C. (1964), *Nature 203*, 687.

Perutz, M. F., Rossman, M. G., Cullis, A. F., Muirhead, H., Will, G., and North, A. C. T. (1960), *Nature 185*, 416.

Rossi-Fanelli, A., Antonini, E., and Caputo, A. (1961), *J. Biol. Chem. 236*, 397.

Rossi-Fanelli, A., Antonini, E., and Caputo, A. (1964), *Advan. Protein Chem. 19*, 73.

Roughton, F. J. W., Otis, A. B., and Lyster, R. L. J., (1955), *Proc. Roy. Soc. (London) B144*, 29.

Schachman, H. K. (1963), *Cold Spring Harbor Symp. Quant. Biol. 28*, 409.

Smith, E. L., and Margoliash, E. (1964), *Federation Proc. 23*, 1243.

Taketa, K., and Pogell, B. M. (1965), *J. Biol. Chem. 240*, 651.

Theorell, H. (1934), *Biochem. Z. 268*, 46.

Umbarger, H. E. (1964), *Science 145*, 674.

Wyman, J. (1964), *Advan. Protein Chem. 19*, 223.